NOT FOR PUBLICATION

NEANDC(J)-125/U
INDC(JPN)-111/U

PROGRESS REPORT

(JULY 1986 TO JUNE 1987 INCLUSIVE)

SEPTEMBER 1987

EDITOR
S. KIKUCHI
JAPANESE NUCLEAR DATA COMMITTEE

JAPAN ATOMIC ENERGY RESEARCH INSTITUTE
TOKAI RESEARCH ESTABLISHMENT
TOKAI-MURA, IBARAKI-KEN, JAPAN

Editor's Note

This is a collection of reports which have been submitted to the Japanese Nuclear Data Committee at the committee's request. The request was addressed to the following individuals who might represent or be in touch with groups doing researches related to the nuclear data of interest to the development of the nuclear energy program.

Although the editor tried not to miss any appropriate addressees, there may have been some oversight. Meanwhile, contribution of a report rested with discretion of its author. The coverage of this document, therefore, may not be uniform over the related field or research.

In this progress report, each individual report is generally reproduced as it was received by the JNDC secretariat, and editor also let pass some simple obvious errors in the manuscripts if any.

This edition covers a period of July 1, 1986 to June 30, 1987. The information herein contained is of a nature of "Private Communication". Data contained in this report should not be quoted without the author's permission.

TABLE OF CONTENTS

ELEMENT S	A	QUANTITY	ENERGY MIN	MAX	LAB	TYPE	DOCUMENTATION REF	VOL	PAGE	DATE	COMMENTS
HE	3	EVALUATION	10-5	20+7	JAE	EVAL-PROG	NEANDC(J)125			SEP 87	SHIBATA.P20.FOR JENDL-3
HE	3	TOTAL	10-5	20+7	JAE	EVAL-PROG	NEANDC(J)125			SEP 87	SHIBATA.P20.FOR JENDL-3,NDG
HE	3	ELASTIC	10-5	20+7	JAE	EVAL-PROG	NEANDC(J)125			SEP 87	SHIBATA.P20.FOR JENDL-3,SIG IN TBL
HE	3	N, PROTON	10-5	20+7	JAE	EVAL-PROG	NEANDC(J)125			SEP 87	SHIBATA.P20.FOR JENDL-3,TBL+FIG GIVN
HE	3	N, DEUTERON	TR	20+7	JAE	EVAL-PROG	NEANDC(J)125			SEP 87	SHIBATA.P20.FOR JENDL-3,NDG
HE	4	EVALUATION	10-5	20+7	JAE	EVAL-PROG	NEANDC(J)125			SEP 87	SHIBATA.P20.FOR JENDL-3
HE	4	TOTAL	10-5	20+7	JAE	EVAL-PROG	NEANDC(J)125			SEP 87	SHIBATA.P20.FOR JENDL-3,SIG IN FIG
HE	4	ELASTIC	10-5	20+7	JAE	EVAL-PROG	NEANDC(J)125			SEP 87	SHIBATA.P20.FOR JENDL-3,R-MATRIX CAL
LI	7	ELASTIC	11+7	13+7	JAE	EXPT-PROG	NEANDC(J)125			SEP 87	CHIBA+.P16.NDG,478 KEV LVL INCLUDED
LI	7	DIFF ELASTIC	11+7	13+7	JAE	EXPT-PROG	NEANDC(J)125			SEP 87	CHIBA+.P16.NDG,478 KEV LVL INCLUDED
LI	7	DIFF INELAST	11+7	13+7	JAE	EXPT-PROG	NEANDC(J)125			SEP 87	CHIBA+.P16.SIG IN FIG OF 4.63MEV LVL
B	10	EVALUATION	10-5	20+7	JAE	EVAL-PROG	NEANDC(J)125			SEP 87	CHIBA.P23.NDG,FOR JENDL-3
B	10	TOTAL	10-5	20+7	JAE	EVAL-PROG	NEANDC(J)125			SEP 87	CHIBA.P23.NDG,FOR JENDL-3
B	10	ELASTIC	10-5	20+7	JAE	EVAL-PROG	NEANDC(J)125			SEP 87	CHIBA.P23.NDG,FOR JENDL-3
B	10	DIFF ELASTIC	10-5	20+7	JAE	EVAL-PROG	NEANDC(J)125			SEP 87	CHIBA.P23.NDG,FOR JENDL-3
B	10	TOT INELAST	TR	20+7	JAE	EVAL-PROG	NEANDC(J)125			SEP 87	CHIBA.P23.NDG,FOR JENDL-3
B	10	DIFF INELAST	TR	20+7	JAE	EVAL-PROG	NEANDC(J)125			SEP 87	CHIBA.P23.NDG,FOR JENDL-3
B	10	N, GAMMA	10-5	20+7	JAE	EVAL-PROG	NEANDC(J)125			SEP 87	CHIBA.P23.NDG,FOR JENDL-3
B	10	N, 2N	TR	20+7	JAE	EVAL-PROG	NEANDC(J)125			SEP 87	CHIBA.P23.NDG,FOR JENDL-3
B	10	N, PROTON	10-5	20+7	JAE	EVAL-PROG	NEANDC(J)125			SEP 87	CHIBA.P23.NDG,FOR JENDL-3

ELEMENT S	A	QUANTITY	ENERGY MIN	MAX	LAB	TYPE	DOCUMENTATION REF	VOL	PAGE	DATE	COMMENTS
B	10	N, DEUTERON	TR	20+7	JAE	EVAL-PROG	NEANDC(J)125			SEP 87	CHIBA.P23.NDG,FOR JENDL-3
B	10	N, TRITON	10-5	20+7	JAE	EVAL-PROG	NEANDC(J)125			SEP 87	CHIBA.P23.NDG,FOR JENDL-3
B	10	N, ALPHA	10-5	20+7	JAE	EVAL-PROG	NEANDC(J)125			SEP 87	CHIBA.P23.NDG,FOR JENDL-3
B	11	EVALUATION	10-5	20+7	JAE	EVAL-PROG	NEANDC(J)125			SEP 87	FUKAHORI.P24.FOR JENDL-3
B	11	TOTAL	10-5	20+7	JAE	EVAL-PROG	NEANDC(J)125			SEP 87	FUKAHORI.P24.FOR JENDL-3,FIG GIVN
B	11	ELASTIC	10-5	20+7	JAE	EVAL-PROG	NEANDC(J)125			SEP 87	FUKAHORI.P24.FOR JENDL-3,NDG
B	11	DIFF ELASTIC	13+7		JAE	EXPT-PROG	NEANDC(J)125			SEP 87	YAMANOUTI+.P18.NDG,TOF,NE213 DET
B	11	DIFF ELASTIC	10-5	20+7	JAE	EVAL-PROG	NEANDC(J)125			SEP 87	FUKAHORI.P24.FOR JENDL-3,FIGS GIVN
B	11	TOT INELAST	23+6	20+7	JAE	EVAL-PROG	NEANDC(J)125			SEP 87	FUKAHORI.P24.FOR JENDL-3,NDG
B	11	DIFF INELAST	13+7		JAE	EXPT-PROG	NEANDC(J)125			SEP 87	YAMANOUTI+.P18.ANGDIST OF 3 LVLS.NDG
B	11	DIFF INELAST	23+6	20+7	JAE	EVAL-PROG	NEANDC(J)125			SEP 87	FUKAHORI.P24.FOR JENDL-3,FIG GIVN
B	11	N, GAMMA	10-5	20+7	JAE	EVAL-PROG	NEANDC(J)125			SEP 87	FUKAHORI.P24.FOR JENDL-3,NDG
B	11	N, 2N	13+7	20+7	JAE	EVAL-PROG	NEANDC(J)125			SEP 87	FUKAHORI.P24.FOR JENDL-3,FIG GIVN
B	11	N, PROTON	12+7	20+7	JAE	EVAL-PROG	NEANDC(J)125			SEP 87	FUKAHORI.P24.FOR JENDL-3,NDG
B	11	N,N PROTON	12+7	20+7	JAE	EVAL-PROG	NEANDC(J)125			SEP 87	FUKAHORI.P24.FOR JENDL-3,NDG
B	11	N, ALPHA	72+6	20+7	JAE	EVAL-PROG	NEANDC(J)125			SEP 87	FUKAHORI.P24.FOR JENDL-3,NDG
B	11	N,N ALPHA	95+6	20+7	JAE	EVAL-PROG	NEANDC(J)125			SEP 87	FUKAHORI.P24.FOR JENDL-3,NDG
C	12	DIFF ELASTIC	14+7		TOH	EXPT-PROG	NEANDC(J)125			SEP 87	BABA+.P77.TOF,NDG
C	12	DIFF INELAST	14+7		TOH	EXPT-PROG	NEANDC(J)125			SEP 87	BABA+.P77.TOF,NDG
C	12	N EMISSION	14+7		TOH	EXPT-PROG	NEANDC(J)125			SEP 87	BABA+.P77.TOF,NDG

ELEMENT S	A	QUANTITY	ENERGY MIN	ENERGY MAX	LAB	TYPE	DOCUMENTATION REF	VOL	PAGE	DATE	COMMENTS
O	16	RESON PARAMS	43+5		TIT	EXPT-PROG	NEANDC(J)125			SEP 87	KITAZAWA+.P90.CONTRIB. TO 87LEUVEN
AL	27	N, PROTON	13+7	15+7	NAG	EXPT-PROG	NEANDC(J)125			SEP 87	KATOH+.P71.ACTIVATION SIG,FIG GIVN
SI	28	RESON PARAMS	57+5	81+5	TIT	EXPT-PROG	NEANDC(J)125			SEP 87	KITAZAWA+.P90.CONTRIB. TO 87LEUVEN
SI	28	RESON PARAMS	57+5		TIT	THEO-PROG	NEANDC(J)125			SEP 87	KITAZAWA+.P87.PUBL. IN NP,A464,61
S	32	RESON PARAMS	10+5	20+5	TIT	EXPT-PROG	NEANDC(J)125			SEP 87	KITAZAWA+.P90.CONTRIB. TO 87LEUVEN
TI		DIFF ELASTIC	14+7		TOH	EXPT-PROG	NEANDC(J)125			SEP 87	BABA+.P77.TOF,NDG
TI		DIFF INELAST	14+7		TOH	EXPT-PROG	NEANDC(J)125			SEP 87	BABA+.P77.TOF,NDG
TI		N EMISSION	14+7		TOH	EXPT-PROG	NEANDC(J)125			SEP 87	BABA+.P77.TOF,DA/DE IN FIG
CU		DIFF ELASTIC	14+7		TOH	EXPT-PROG	NEANDC(J)125			SEP 87	BABA+.P77.TOF,NDG
CU		DIFF INELAST	14+7		TOH	EXPT-PROG	NEANDC(J)125			SEP 87	BABA+.P77.TOF,NDG
CU		N EMISSION	14+7		TOH	EXPT-PROG	NEANDC(J)125			SEP 87	BABA+.P77.TOF,DA/DE IN FIG
CU	63	N, 2N	13+7	15+7	NAG	EXPT-PROG	NEANDC(J)125			SEP 87	KATOH+.P71.ACTIVATION SIG,FIG GIVN
ZR		DIFF ELASTIC	14+7		TOH	EXPT-PROG	NEANDC(J)125			SEP 87	BABA+.P77.CFD KALBACK-MANN'S THEORY
ZR		DIFF INELAST	14+7		TOH	EXPT-PROG	NEANDC(J)125			SEP 87	BABA+.P77.CFD KALBACK-MANN'S THEORY
ZR		N EMISSION	14+7		TOH	EXPT-PROG	NEANDC(J)125			SEP 87	BABA+.P77.TOF,DA/DE IN FIG
AG		EVALUATION	10-5	20+7	JAE	EVAL-PROG	NEANDC(J)125			SEP 87	LIU+.P28.FOR JENDL-3
AG		TOTAL	10-5	20+7	JAE	EVAL-PROG	NEANDC(J)125			SEP 87	LIU+.P28.FOR JENDL-3,NDG
AG		ELASTIC	10-5	20+7	JAE	EVAL-PROG	NEANDC(J)125			SEP 87	LIU+.P28.FOR JENDL-3,NDG
AG		DIFF ELASTIC	10-5	20+7	JAE	EVAL-PROG	NEANDC(J)125			SEP 87	LIU+.P28.FOR JENDL-3,NDG
AG		TOT INELAST	TR	20+7	JAE	EVAL-PROG	NEANDC(J)125			SEP 87	LIU+.P28.FOR JENDL-3,NDG

ELEMENT S	A	QUANTITY	ENERGY MIN	MAX	LAB	TYPE	DOCUMENTATION REF	VOL	PAGE	DATE	COMMENTS
AG		DIFF INELAST	TR	20+7	JAE	EVAL-PROG	NEANDC(J)125			SEP 87	LIU+.P28.FOR JENDL-3,NDG
AG		N, GAMMA	10-5	20+7	JAE	EVAL-PROG	NEANDC(J)125			SEP 87	LIU+.P28.FOR JENDL-3,NDG
AG		NONELA GAMMA	10-5	20+7	JAE	EVAL-PROG	NEANDC(J)125			SEP 87	LIU+.P28.FOR JENDL-3,NDG
AG		N, 2N	TR	20+7	JAE	EVAL-PROG	NEANDC(J)125			SEP 87	LIU+.P28.FOR JENDL-3,NDG
AG		N, XN X>2	TR	20+7	JAE	EVAL-PROG	NEANDC(J)125			SEP 87	LIU+.P28.(N,3N),FOR JENDL-3,NDG
AG		N EMISSION	14+7		KYU	EXPT-PROG	NEANDC(J)125			SEP 87	WATANABE+.P62.ANG-E DIST.FIG GIVN
AG		N, PROTON	TR	20+7	JAE	EVAL-PROG	NEANDC(J)125			SEP 87	LIU+.P28.FOR JENDL-3,NDG
AG		N,N PROTON	TR	20+7	JAE	EVAL-PROG	NEANDC(J)125			SEP 87	LIU+.P28.FOR JENDL-3,NDG
AG		N, ALPHA	10-5	20+7	JAE	EVAL-PROG	NEANDC(J)125			SEP 87	LIU+.P28.FOR JENDL-3,NDG
AG		N,N ALPHA	TR	20+7	JAE	EVAL-PROG	NEANDC(J)125			SEP 87	LIU+.P28.FOR JENDL-3,NDG
AG	107	EVALUATION	10-5	20+7	JAE	EVAL-PROG	NEANDC(J)125			SEP 87	LIU+.P28.FOR JENDL-3
AG	107	TOTAL	10-5	20+7	JAE	EVAL-PROG	NEANDC(J)125			SEP 87	LIU+.P28.FOR JENDL-3,NDG
AG	107	ELASTIC	10-5	20+7	JAE	EVAL-PROG	NEANDC(J)125			SEP 87	LIU+.P28.FOR JENDL-3,NDG
AG	107	DIFF ELASTIC	10-5	20+7	JAE	EVAL-PROG	NEANDC(J)125			SEP 87	LIU+.P28.FOR JENDL-3,NDG
AG	107	TOT INELAST	TR	20+7	JAE	EVAL-PROG	NEANDC(J)125			SEP 87	LIU+.P28.FOR JENDL-3,NDG
AG	107	DIFF INELAST	TR	20+7	JAE	EVAL-PROG	NEANDC(J)125			SEP 87	LIU+.P28.FOR JENDL-3,FIGS GIVN
AG	107	N, GAMMA	10-5	20+7	JAE	EVAL-PROG	NEANDC(J)125			SEP 87	LIU+.P28.FOR JENDL-3,FIG GIVN
AG	107	NONELA GAMMA	10-5	20+7	JAE	EVAL-PROG	NEANDC(J)125			SEP 87	LIU+.P28.FOR JENDL-3,NDG
AG	107	N, 2N	TR	20+7	JAE	EVAL-PROG	NEANDC(J)125			SEP 87	LIU+.P28.FOR JENDL-3,NDG
AG	107	N, XN X>2	TR	20+7	JAE	EVAL-PROG	NEANDC(J)125			SEP 87	LIU+.P28.(N,3N),FOR JENDL-3,NDG

ELEMENT S	A	QUANTITY	ENERGY MIN	MAX	LAB	TYPE	DOCUMENTATION REF	VOL	PAGE	DATE	COMMENTS
AG	107	N, PROTON	TR	20+7	JAE	EVAL-PROG	NEANDC(J)125			SEP 87	LIU+.P28.FOR JENDL-3,NDG
AG	107	N,N PROTON	TR	20+7	JAE	EVAL-PROG	NEANDC(J)125			SEP 87	LIU+.P28.FOR JENDL-3,NDG
AG	107	N, ALPHA	10-5	20+7	JAE	EVAL-PROG	NEANDC(J)125			SEP 87	LIU+.P28.FOR JENDL-3,NDG
AG	107	N,N ALPHA	TR	20+7	JAE	EVAL-PROG	NEANDC(J)125			SEP 87	LIU+.P28.FOR JENDL-3,NDG
AG	109	EVALUATION	10-5	20+7	JAE	EVAL-PROG	NEANDC(J)125			SEP 87	LIU+.P28.FOR JENDL-3
AG	109	TOTAL	10-5	20+7	JAE	EVAL-PROG	NEANDC(J)125			SEP 87	LIU+.P28.FOR JENDL-3,NDG
AG	109	ELASTIC	10-5	20+7	JAE	EVAL-PROG	NEANDC(J)125			SEP 87	LIU+.P28.FOR JENDL-3,NDG
AG	109	DIFF ELASTIC	10-5	20+7	JAE	EVAL-PROG	NEANDC(J)125			SEP 87	LIU+.P28.FOR JENDL-3,NDG
AG	109	TOT INELAST	TR	20+7	JAE	EVAL-PROG	NEANDC(J)125			SEP 87	LIU+.P28.FOR JENDL-3,NDG
AG	109	DIFF INELAST	TR	20+7	JAE	EVAL-PROG	NEANDC(J)125			SEP 87	LIU+.P28.FOR JENDL-3,NDG
AG	109	N, GAMMA	10-5	20+7	JAE	EVAL-PROG	NEANDC(J)125			SEP 87	LIU+.P28.FOR JENDL-3,FIG GIVN
AG	109	NONELA GAMMA	10-5	20+7	JAE	EVAL-PROG	NEANDC(J)125			SEP 87	LIU+.P28.FOR JENDL-3,NDG
AG	109	N, 2N	TR	20+7	JAE	EVAL-PROG	NEANDC(J)125			SEP 87	LIU+.P28.FOR JENDL-3,NDG
AG	109	N, XN X>2	TR	20+7	JAE	EVAL-PROG	NEANDC(J)125			SEP 87	LIU+.P28.(N,3N),FOR JENDL-3,NDG
AG	109	N, PROTON	TR	20+7	JAE	EVAL-PROG	NEANDC(J)125			SEP 87	LIU+.P28.FOR JENDL-3,NDG
AG	109	N,N PROTON	TR	20+7	JAE	EVAL-PROG	NEANDC(J)125			SEP 87	LIU+.P28.FOR JENDL-3,NDG
AG	109	N, ALPHA	10-5	20+7	JAE	EVAL-PROG	NEANDC(J)125			SEP 87	LIU+.P28.FOR JENDL-3,NDG
AG	109	N,N ALPHA	TR	20+7	JAE	EVAL-PROG	NEANDC(J)125			SEP 87	LIU+.P28.FOR JENDL-3,NDG
CD		N EMISSION	14+7		KYU	EXPT-PROG	NEANDC(J)125			SEP 87	WATANABE+.P62.ANG-E DIST.FIG GIVN
IN		N EMISSION	14+7		KYU	EXPT-PROG	NEANDC(J)125			SEP 87	WATANABE+.P62.ANG-E DIST.FIG GIVN

ELEMENT S	A	QUANTITY	ENERGY MIN	MAX	LAB	TYPE	DOCUMENTATION REF VOL PAGE	DATE	COMMENTS
SN		N EMISSION	14+7		KYU	EXPT-PROG	NEANDC(J)125	SEP 87	WATANABE+.P62.ANG-E DIST.FIG GIVN
SB		N EMISSION	14+7		KYU	EXPT-PROG	NEANDC(J)125	SEP 87	WATANABE+.P62.ANG-E DIST.FIG GIVN
TE		N EMISSION	14+7		KYU	EXPT-PROG	NEANDC(J)125	SEP 87	WATANABE+.P62.ANG-E DIST.FIG GIVN
BA	135	RESON PARAMS	40+2	46+3	JAE	EXPT-PROG	NEANDC(J)125	SEP 87	MIZUMOTO.P19.SUBMITTED TO NST
BA	135	STRNTH FNCTN	40+2	46+3	JAE	EXPT-PROG	NEANDC(J)125	SEP 87	MIZUMOTO.P19.SUBMITTED TO NST
BA	137	RESON PARAMS	40+2	15+3	JAE	EXPT-PROG	NEANDC(J)125	SEP 87	MIZUMOTO.P19.SUBMITTED TO NST
BA	137	RESON PARAMS	40+2	15+3	JAE	EXPT-PROG	NEANDC(J)125	SEP 87	MIZUMOTO.P19.SUBMITTED TO NST
BA	138	RESON PARAMS	40+2	63+3	JAE	EXPT-PROG	NEANDC(J)125	SEP 87	MIZUMOTO.P19.SUBMITTED TO NST
ND	144	N, 2N	TR	20+7	JAE	EVAL-PROG	NEANDC(J)125	SEP 87	JNDC.P35.EVAP MDL CAL,FIG GIVN
ND	146	N, 2N	TR	20+7	JAE	EVAL-PROG	NEANDC(J)125	SEP 87	JNDC.P35.EVAP MDL CAL,FIG GIVN
ND	148	N, 2N	TR	20+7	JAE	EVAL-PROG	NEANDC(J)125	SEP 87	JNDC.P35.EVAP MDL CAL,FIG GIVN
ND	150	N, 2N	TR	20+7	JAE	EVAL-PROG	NEANDC(J)125	SEP 87	JNDC.P35.EVAP MDL CAL,FIG GIVN
EU	154	RES INT ABS	NDG		JAE	EXPT-PROG	NEANDC(J)125	SEP 87	SEKINE+.P11.PUBLISHED IN ARI,38,513
EU	154	N, GAMMA	PILE		JAE	EXPT-PROG	NEANDC(J)125	SEP 87	SEKINE+.P11.PUBLISHED IN ARI,38,513
EU	155	RES INT ABS	NDG		JAE	EXPT-PROG	NEANDC(J)125	SEP 87	SEKINE+.P11.PUBLISHED IN ARI,38,513
EU	155	N, GAMMA	PILE		JAE	EXPT-PROG	NEANDC(J)125	SEP 87	SEKINE+.P11.PUBLISHED IN ARI,38,513
TH	232	SPECT FISS N	20+6		TOH	EXPT-PROG	NEANDC(J)125	SEP 87	BABA+.P80.TOF,NE213 DTCTR.FIG GIVN
U	233	FISSION	20+5	80+5	TOH	EXPT-PROG	NEANDC(J)125	SEP 87	MANABE+.P81.REL TO U235.FIG CFD OTHR
U	235	FISSION	14+7	15+7	TOH	EXPT-PROG	NEANDC(J)125	SEP 87	KARINO+.P82.ABSL.FIG CFD OTHER WORKS
AM	243	FISSION	11+6	68+6	TOH	EXPT-PROG	NEANDC(J)125	SEP 87	KANDA+.P83.PUBLISHED IN NST,24,423

ELEMENT S A	QUANTITY	ENERGY MIN	ENERGY MAX	LAB	TYPE	DOCUMENTATION REF VOL PAGE	DATE	COMMENTS
BK 250	EVALUATION	10-5	20+7	JAE	EVAL-PROG	NEANDC(J)125	SEP 87	NAKAGAWA.P31.FOR JENDL-3,NDG
CF 252	EVALUATION	10-5	20+7	JAE	EVAL-PROG	NEANDC(J)125	SEP 87	NAKAGAWA.P31.FOR JENDL-3,NDG
MANY	EVALUATION	10-5	20+7	JAE	EVAL-PROG	NEANDC(J)125	SEP 87	JNDC.P35.172 FP NUCLIDES FOR JENDL-3
MANY	EVALUATION	10-5	20+7	JAE	EVAL-PROG	NEANDC(J)125	SEP 87	JNDC.P39.21 ACTINIDES FOR JENDL-3
MANY	SPECT N,GAMM	+4	+5	TIT	EXPT-PROG	NEANDC(J)125	SEP 87	IGASHIRA+.P89.CONTRIB. TO 87LEUVEN
MANY	N, 2N	FISS		KNK	THEO-PROG	NEANDC(J)125	SEP 87	HORIBE.P45.EMPIRICAL RULE,TBL GIVN

The content table in the CINDA format was compiled by the JNDC CINDA group;

S. Chiba (JAERI), M. Kawai (NAIG),
H. Kitazawa (Tokyo Inst. of Tech.), T. Nakagawa (JAERI),
R. Nakasima (Hosei Univ.), M. Sakamoto (JAERI).

I. ELECTROTECHNICAL LABORATORY

Quantum Technology Division

I-1 International Intercomparison of Monoenergetic Neutron Fluence by Using ^{235}U and ^{238}U Fission Chambers

K.Kudo, T.Kinoshita, A.Fukuda, N.Kobayashi
and K.Takeuchi*

After the first series of international intercomparisons on monoenergetic neutron fluences in the energy range from 250 keV to 14.8 MeV had been carried out under the auspices of the Section III (neutron measurements) of the Consultative Committee for Measurement Standards of Ionizing Radiations (CCEMRI), the second series of intercomparisons is in progress by using transfer instruments based on activation techniques such as $^{115}In(n,\gamma)^{116}In$, $^{115}In(n,n')^{115m}In$ and $^{90}Zr(n,2n)/^{93}Nb(n,2n)$ reactions and on counting techniques by the use of ^{235}U and ^{238}U fission chambers. The Electrotechnical Laboratory (ETL) has participated in the intercomparisons summarized in Table 1.

The intercomparisons based on the fission chambers were proposed to adopt cross section measurements as a trasfer technique, and Atomic

---

* Ship Research Institute

Energy Research Establishment (AERE Harwell, co-ordinator D.B.Gayther) supplied gas-flow type chambers of ^{235}U and ^{238}U, and they were circulated to about 10 participants in sequence. After each calibration the chambers were carefully inspected the pulse height and the efficiency under controlled conditions with the same ^{252}Cf neutron source, which was recalibrated at National Physical Laboratory (NPL Teddington) on each occasion. Intercomparison for the neutron energy at 0.144 MeV was added to the energy points to introduce another participants using reactor filtered beams.

The chambers sent from AERE in the middle of 1986 were calibrated in the standards fields of ETL. A 4 MV Pelletron was used for producing monoenergetic neutrons at 0.144, 0.565 and 5.0 MeV and a 300 kV Cockcroft-Walton type accelerator was employed at 14.6 MeV. The chambers were irradiated at distances from 60 to 75 cm from a neutron source. The layout for the measurement is shown in Fig. 1.

Methods for neutron fluence measurements adopted in the calibration are shown in Table 2. For neutron fluence measurements at 0.144 MeV, a H_2 spherical counter was adopted to measure the hydrogen recoil spectrum, which was fitted with the one based on a Monte-Carlo calculation(1), and the result is shown in Fig. 2. Mckibben and Pangher type Long counters were used as fluence monitors during the irradiation except for the case of 14.6 MeV calibration with the use of an associated α particle method.

Scattered and induced neutrons from both the target assembly and the surroundings are difficult to estimate and cause a major uncertainty in the result. The energy spectra at the chamber position were calculated by a two-dimensional discrete-ordinates transport code PALLAS(2) with the neutron cross sections processed from the ENDF/B-IV. An example of the calculated spectrum in the case of 14.6 MeV irradiation is shown in Fig. 3.

The calibration work performed in ETL has been already finished and the results of the intercomparisons would be published shortly after by the co-ordinator.

References

(1) N.Kobayashi et al.: Nucl. Instr. Meth., **A242**, 164 (1985).

(2) K.Takeuchi et al.: JAERI-M 84-244 (1985).

transfer instruments	En(MeV) 0.144	0.250	0.565	2.5	5.0	14.6
Bonner sphere		x	x	x		
^{3}He counter		x	x			
$^{115}In(n,\gamma)^{115}In$	x	x				
$^{115}In(n,n')^{115m}In$				x		x
90Zr(n,2n) and 93Nb(n,2n)						x
^{235}U fission ch.	x		x		x	x
^{238}U fission ch.					x	x

Table 1. International intercomparisons in which ETL has participated.

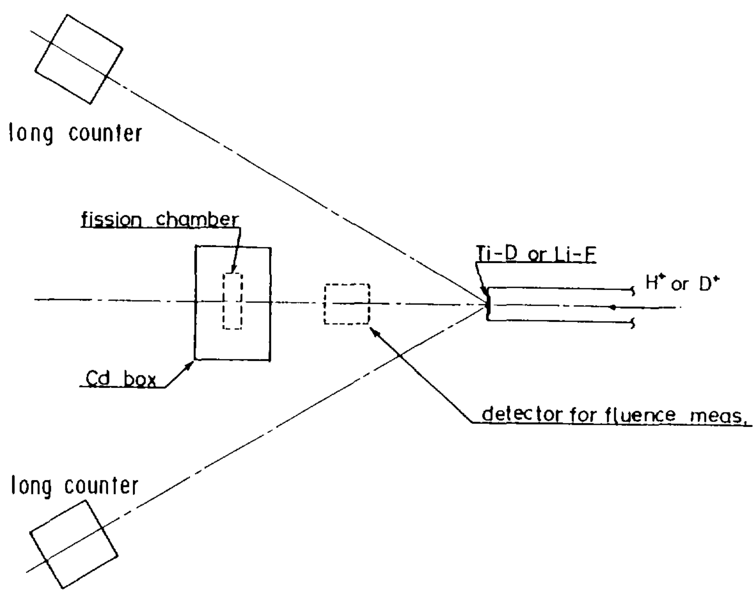

Figure 1. The layout of the measurements at 0.144, 0.565 and 5.0 MeV.

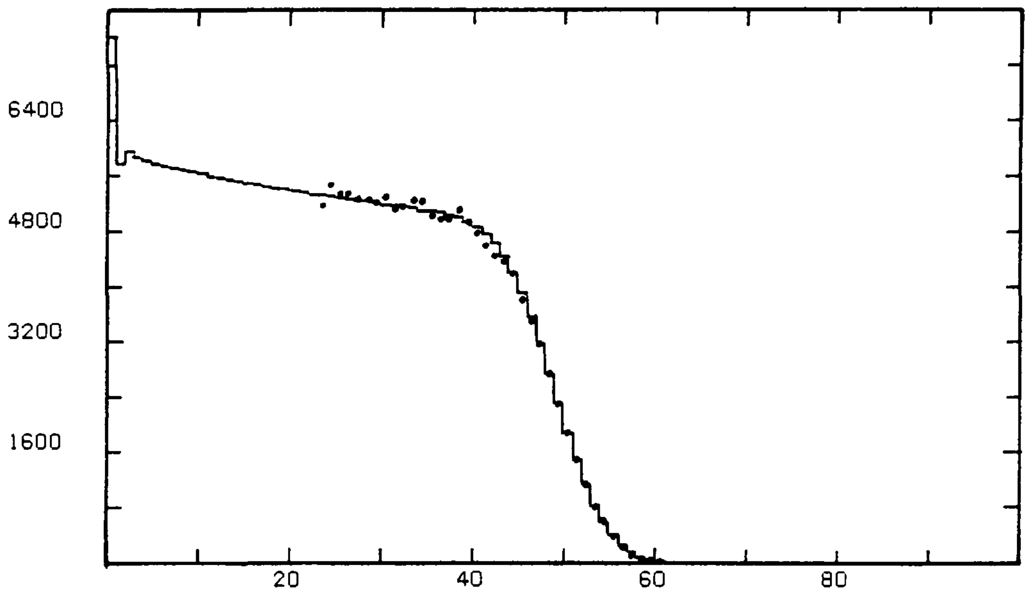

Figure 2. Pulse height spectrum(dotted line) measured by a H_2 sherical counter with the calculated one(solid line).

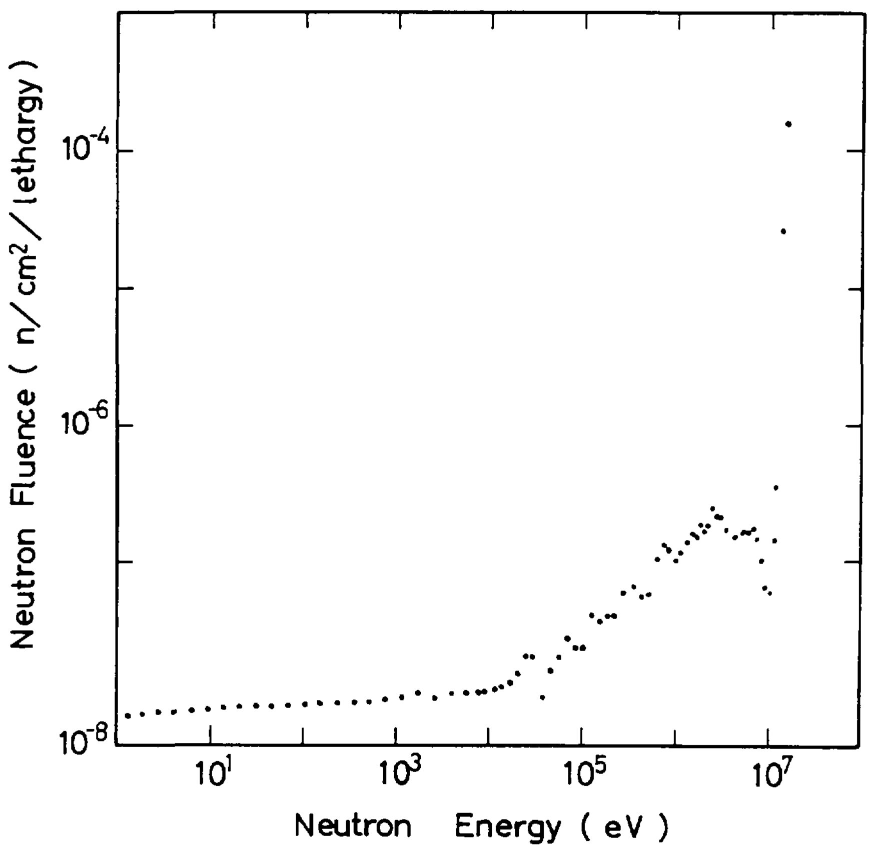

Figure 3. Direct and indirect neutron spectrum at 14.6 MeV neutron calibration at the position of the chamber calculated by PALLAS.

II. Japan Atomic Energy Research Institute

A. Isotope Research and Development Division

Department of Radioisotopes

II-A-1 Triple Neutron Capture of ^{153}Eu in a Reactor: The Cross Sections of ^{154}Eu and ^{155}Eu

T. Sekine, S. Ichikawa and S. Baba

A paper on this subject has been published in Journal of Appl. Radiat. Isot. 38, pp. 513-516(1987) with an abstract as follows:

Successive neutron captures of ^{153}Eu have been studied by means of an activation method. Samples of ^{153}Eu enriched to 99.9% were irradiated in different reactor neutron spectra. The γ rays associated with the decays of ^{154}Eu, ^{155}Eu and ^{156}Eu produced respectively by one-, two-, and three-neutron captures of ^{153}Eu were recorded and thermel neutron cross sections as well as resonance integrals were calculated for the reactions $^{154}Eu(n,\gamma)^{155}Eu$ (σ_0=(1840±90)barn I_0'=(2100±2100)barn) and $^{155}Eu(n,\gamma)^{156}Eu$ (σ_0=(3760±170)barn I_0'=(15300±2700)barn).

II-A-2 Decay Spectroscopy of ^{130}Pr, ^{128}Pr, ^{124}La, ^{122}La and the new Isotope ^{121}La

T. Sekine, K. Hata, Y. Nagame, S. Ichikawa,
H. Iimura, M. Oshima, N. Takahashi* and A. Yokoyama*

Decays of neutron deficient isotopes of lanthanum and praseodymium have been studied using heavy-ion reactions and on-line mass separation. For this purpose, we have developed mass separation of molecular beams for lifgt rare-earth elements to strengthen elemental selectivity.

A 4.1 mg/cm^2 thick Mo foil with natural isotopic abundances and a 3.8 mg/cm^2 thick ^{103}Rh foil were bombarded with ^{32}S beams for production of the Pr and the La isotopes, respectively. The reaction products were ionized with a thermal ion source. The La isotopes were obtained as monoxide ions (LaO^+) to be separated from their Cs and Ba isobars. On the other hand, the Pr isotopes were obtained as metalic ions, being separated from their Ce and La isobars.

The mass-separated products were implanted into an aluminum coated Mylar tape in front of two Ge(HP) detectoes for γ-γ coincidence measurement. After collecting for a preselected time period, the activity was transported within 1 sec into the counting position, equipped with a 2-mm thick plastic scintillator for β detection and a Ge(HP) detector for γ detection.

---

* Faculty of Science, Osaka University

From the mass-separated sources, we have obtained β-coincident γ-ray spectra for A=130, 128, 140($^{124}LaO^+$) and 138 ($^{122}LaO^+$), as shown in Fig.1. All the spectra in Fig.1 show prominent $2^+ \rightarrow 0^+$ and $4^+ \rightarrow 2^+$ transitions in their daughter nuclei. In the decays of both ^{128}Pr and ^{122}La, no other transitions were obtained. This means that their ground-state spins are possibly as small as 3. On the other hand, the ground-state spins of ^{130}Pr and ^{124}La must be higher, since in their daughter nuclei are populated such high spin states as 6^+ state for ^{130}Pr and 10^- state for ^{124}La. Constraction of the decay schemes is in progress.

Fig.2 shows the β-time spectrum obtained at A=137. From the spectrum corrected for the background a half-life of 8±2 sec was deduced. The possible sources for the β ray are restricted to $^{121}LaO^+$ and $^{121}CeO^+$, since the compound nuclei are $^{132-x}Ce$, and no fission reaction is expected to occure in the interaction between the ^{32}S beam and a ^{nat}Ta target, which was acting as a catcher. The possibility of $^{121}CeO^+$ as a main source of the β-ray, however, was eliminated because of its small formation cross section in the reaction ^{32}S + ^{92}Mo that was calculated by ALICE code[1)] to be 0.07 mb (8 mb for ^{121}La). In addition, the gross theory[2)] of β decay supports ^{121}La rather than ^{121}Ce; it predicts the half-lives to be 5 sec for ^{121}La and to be 1 sec for ^{121}Ce. From these arguments, we have assigned the 8±2 sec β-ray to the new isotope ^{121}La.

The report of this work is in preparation.

References

1) M. Blann and J. Bisplinghoff: COO-3494-27 (1975)
2) T. Takahashi, M. Yamada and T. Kondoh: At. Nucl. Data Tables 12 (1973) 101

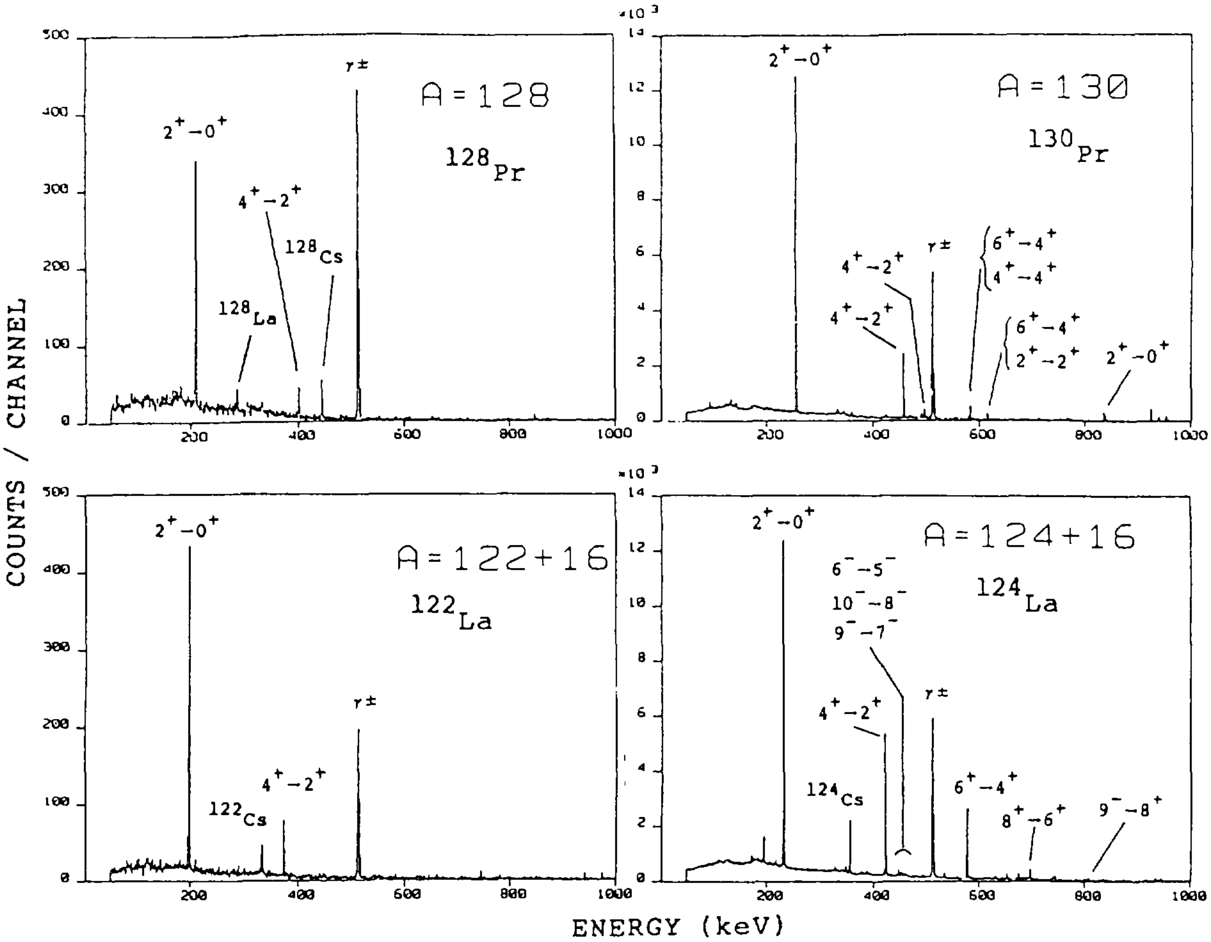

Fig.1 β-coincident γ-ray spectra obtained at A=128 and 130 in the reaction ^{32}S + ^{103}Rh, and at A=138 and 140 in the reaction ^{32}S + ^{nat}Mo.

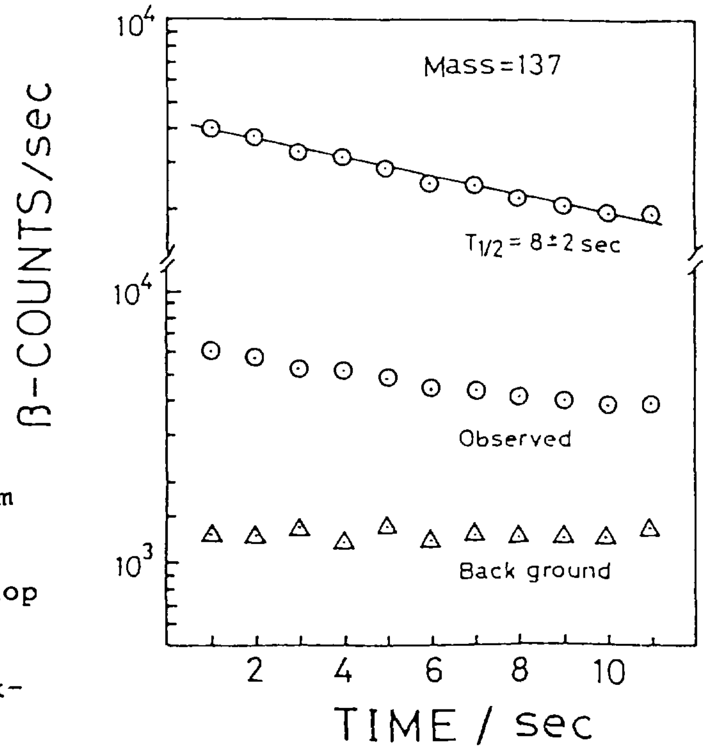

Fig.2 β time spectrum obtained at A=137 ($^{121}LaO^+$). At the top the spectrum corrected for the backgound is plotted.

B. Linac Laboratory, Department of Physics

II-B-1

Neutron Sources with Lithium Target

Y. Yamanouti

A paper on this subject was presented at the IAEA Advisory Group Meeting on Properpies of Neutron Sources held in Leningrad, USSR, 9-13 June, 1986 and published in IAEA-TECDOC-410, Vienna, 1987 with the following abstract.

The $^{7}Li(p,n)^{7}Be$ reaction is widely used as a source of monoenergetic neutrons. Usefulness of the $^{7}Li(p,n)^{7}Be$ reaction as a monoenergetic neutron source can be evaluated from the characteristics on zero-degree energy spectra, zero-degree cross sections, angular distributions, and total reaction cross section of the reaction.The $^{7}Li(p,n)^{7}Be$ reaction on a thin lithium target is the most practical source of monoenergetic neutrons with neutron energy spread of about 400 KeV at proton energies above 30 MeV.

It is also to be noticed that the $^{7}Li + p$ and $^{7}Li + d$ reactions on thick lithium targets are useful sources of intense neutron beams for applications where the monoenergetic characteristics are not required. In these reactions the $^{7}Li + d$ reaction produces the zero-degree neutron yield higher than the $^{7}Li + p$ reaction at the same projectile energy.

In this paper characteristics of the $^{7}Li(p,n)^{7}Be$ reaction as a monoenergetic neutron source and production of intense neutron beams from the $^{7}Li + p$ and $^{7}Li + d$ reactions are presented.

II-B-2

Measurement of the fast neutron scattering cross sections of ^{7}Li at 11.0 and 13.0 MeV

S. Chiba, Y. Yamanouti, M. Mizumoto, M. Hyakutake[*1] and S. Iwasaki[*2]

The fast neutron elastic and inelastic scattering cross sections of ^{7}Li have been measured using the JAERI tandem fast neutron time-of-flight spectrometer at incident energies of 11.0 and 13.0 MeV.

The source neutrons were produced by the $D(d,n)^{3}He$ reaction. The target D_2 gas was contained in a 3-cm long cell with pressure of about 2.0 atms. The scatterer was an enriched metal cylinder of ^{7}Li, 3.1cm in diameter and 4-cm high. The neutron detectors were NE213 liquid scintillator, 20cm in diameter and 35-cm thick, viewed by photomultiplier tubes at both ends. Absolute scale of the cross section and relative detection efficiency were determined by the H(n,n) cross section. Measurements without the target D_2 gas were also performed to subtract a background coming from the neutron source itself. The angular distributions for the elastic plus 1st excited state (0.478 MeV) and the 2nd level (4.63 MeV) were deduced.

In Fig.1, the angle-integrated cross sections for the 2nd state of ^{7}Li are shown. The present results are smaller than the data of Hogue et al.[1)] and JENDL-3PR2 evaluation by about 30%.

1) H.H.Hogue et al., Nucl. Sci. Eng. 69, 22(1979)

---

*1 : Faculty of Engineering, Kyushu University

*2 : Faculty of Engineering, Tohoku University

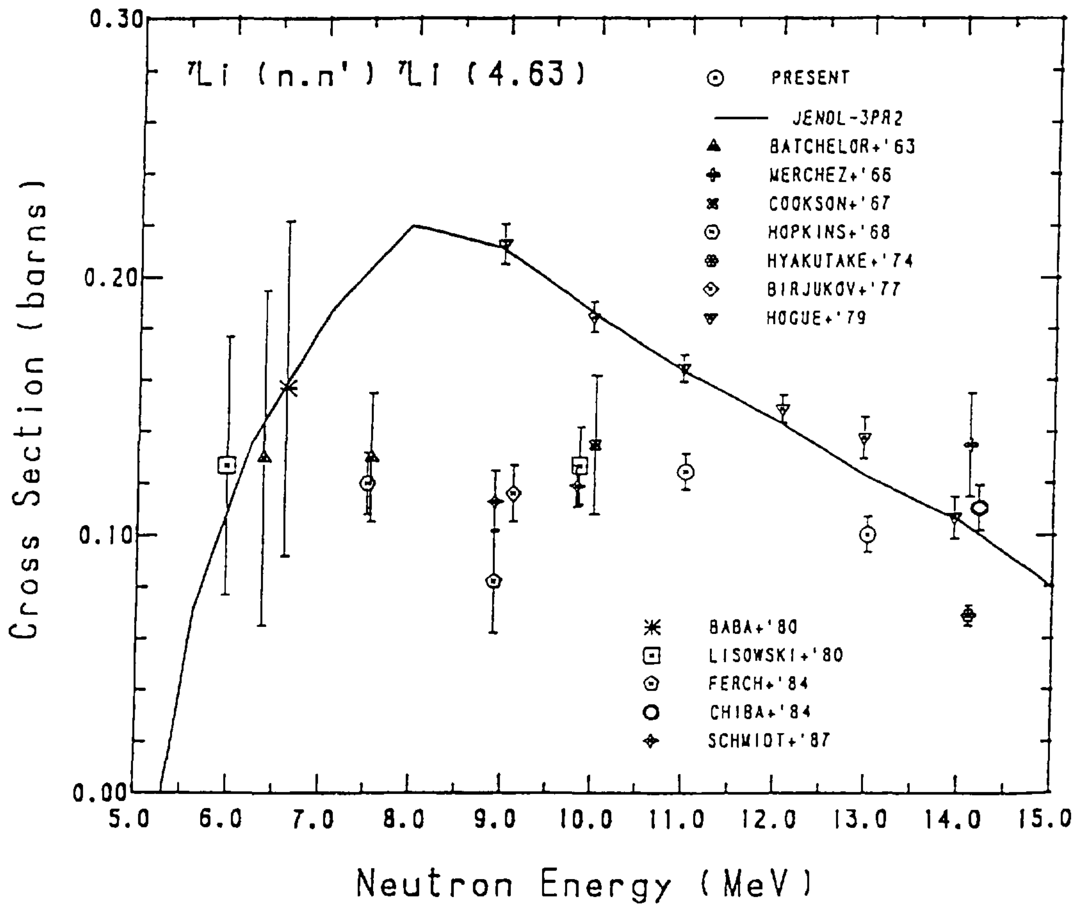

Fig. 1 Angle-integrated neutron inelastic scattering cross section for the 4.63-MeV state of ^{7}Li.

II-B-3 Scattering of 13.0 MeV Neutrons from ^{11}B

Y.Yamanouti, M.Sugimoto, Y.Furuta, M.Mizumoto, M.Hyakutake*
and T.Methasiri**

Differential cross sections for the scattering of 13.0 MeV neutrons from ^{11}B were measured in order to study the reaction mechanism for the neutron scattering on light nuclei in the energy region above 10 MeV. Scattered neutrons were observed by a time-of-flight spectrometer with an array of four 20 cmϕ x 35 cm NE213 liquid scintillator detectors. The JAERI tandem accelerator provided a pulsed deuteron beam to generate monoenergetic neutrons by the $^{2}H(d,n)^{3}He$ reaction.Neutron time-of-flight spectra were taken at scattering angles from 20° to 140°. Inelastic scattering cross sections of neutrons leading to the $1/2^-$ state at 2.125 MeV, the $5/2^-$ state at 4.445 MeV and the $3/2^-$ state at 5.021 MeV were measured simultaneously with the elastic scattering cross sections. The present result of the scattering cross sections is in the same trend as the data obtained by the TUNL group.

* Department of Nuclear Engineering, Kyushu University

** Department of Physics, Chulalongkorn University

II-B-4 Neutron Resonance Parameters of ^{135}Ba, ^{137}Ba and ^{138}Ba

Motoharu Mizumoto

A paper on this subject, which includes the revised data and more detailed information than in Ref (1), has been submitted to J. Nucl. Sci. Technol. with an abstract as follows:

Neutron transmission measurements were carried out on the separated isotopes of Barium at the Japan Atomic Energy Research Institute electron linear accelerator. Resonance energies and neutron widths were determined for a large number of resonances in the neutron energy range from 400 eV to 4.6 keV for ^{135}Ba, to 15 keV for ^{137}Ba and 63 keV for ^{138}Ba. The s-wave strength functions were obtained to be; $S_0 = (1.33 \pm 0.22) \times 10^{-4}$ for ^{135}Ba, and $S_0 = (0.51 \pm 0.12) \times 10^{-4}$ for ^{137}Ba. An apparent energy dependence of the strength function for ^{135}Ba was observed. New resonance parameters of ^{138}Ba for several weak p-wave levels were also obtained.

Reference

(1) M. Mizumoto et al., Proc. Int. Conf. on Nucl. Data for Baic and Applied Sci. Santa Fe , 1985, p533

C. Nuclear Data Center, Department of Physics and Working Groups of Japanese Nuclear Data Committee

II-C-1 Evaluation of Neutron Nuclear Data for ^{3}He and ^{4}He

Keiichi SHIBATA

Neutron nuclear data of ^{3}He and ^{4}He were evaluated for JENDL-3 in the energy range of 10^{-5} eV to 20 MeV. Evaluated quantities are the total, elastic scattering, (n,p) and (n,d) reaction cross sections of ^{3}He, and the total and elastic scattering cross sections of ^{4}He.

As for ^{3}He, the total, elastic scattering and (n,p) reaction cross sections were analyzed by the R-matrix theory below 1 MeV. The calculated thermal cross sections are consistent with the values recommended by Mughaghab et al.[1], as seen in Table 1. Above 1 MeV, the total, (n,p) and (n,d) reaction cross sections were based on available experimental data, and the elastic scattering cross section was obtained by subtracting the reaction cross section from the total cross section Figure 1 shows the evaluated (n,p) reaction cross section.

Concerning ^{4}He, the evaluation was performed by using the R-matrix theory in the overall energy region. The R-matrix calculation reproduces experimental data very well. The total cross section is illustrated in Fig. 2.

References:

1) Mughabghab, S.F. et al. : "Neutron Cross Sections, Vol.1, Part A", Academic Press, (1981).

Table 1 Thermal cross sections of ^{3}He

	Present Work	ENDF/B-V	Mughabghab et al.
elastic	3.1346 b	1.0000 b	3.10 ± 0.13 b
(n,p)	5328.0 b	5327.0 b	5333 ± 7 b

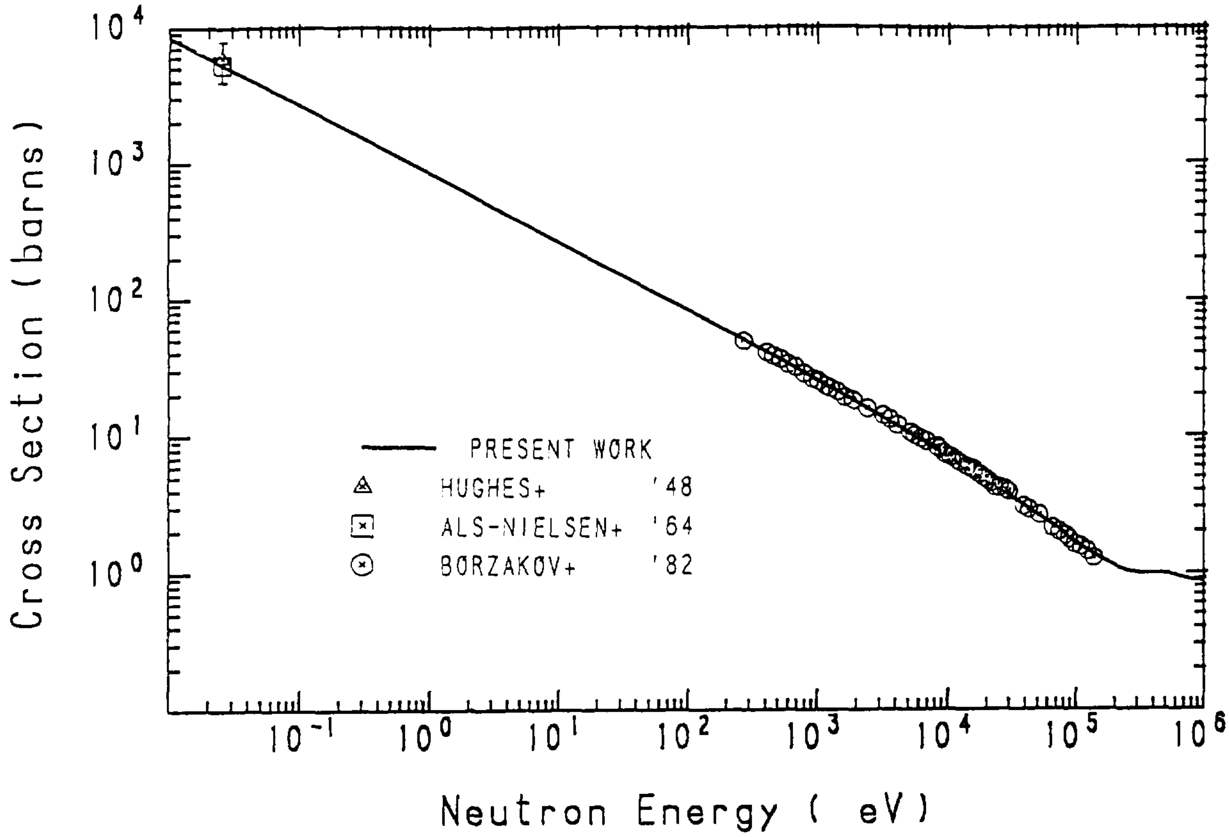

Fig. 1 ^{3}He (n,p) cross section below 1 MeV.

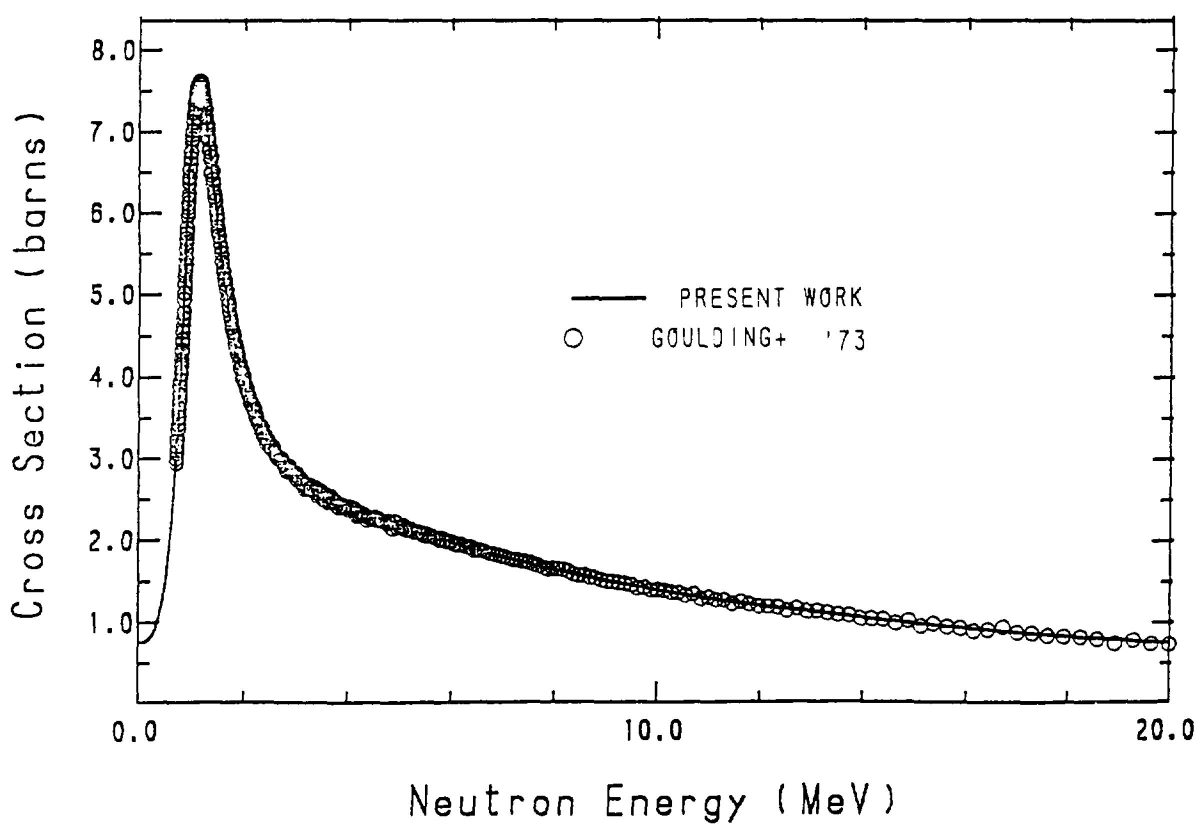

Fig. 2 Total cross section of ^{4}He.

II-C-2 Evaluation of the neutron nuclear data of ^{10}B

Satoshi Chiba

The neutron nuclear data of ^{10}B have been evaluated in the energy range between 10^{-5} eV and 20 MeV. Evaluated are the total, elastic and inelastic scattering, (n,2n), (n,γ), (n,p), (n,d), (n,t)2α and (n,α) reaction cross sections and angular and energy distributions of emitted neutrons. The present evaluation is mainly based on available experimental data.

The total cross section was the sum of the partial cross sections below 1 MeV. Above 1 MeV, the data measured by Auchampahgh et al.[1] were mainly adopted.

The present (n,α) reaction cross section is very close to the data in ENDF/B-V below 100 keV; the 2200m/s-value of 3837 barns, evaluated by Mughabghab et al.[2], was adopted. From 100 keV to 1 MeV, however, the present (n,α_0) cross section is based on the experimental data of Olson et al[3], which are higher than the ENDF/B-V evaluation by as much as 30%.

1) G.F.Auchampaugh et al.: Nucl. Sci. Eng. 69, 30(1979).

2) S.F.Mughabghab et al.: "Neutron Cross Sections", Vol. 1, Part A, Academic Press, 1981.

3) M.D.Olson and R.W.Kavanagh: Phys. Rev. C, 30, 1375(1984)

II-C-3 Evaluation of Neutron Nuclear Data for ^{11}B

Tokio FUKAHORI

Nuclear data of ^{11}B have been evaluated in the energy range from 10^{-5} eV to 20 MeV. The evaluated quantities are shown in Table 1. The evaluation has been performed by using R-matrix code RESCAL[1] below 7 MeV and multistep statistical model code TNG[2,3] above 7 MeV. Below 7 MeV, R-matrix parameters of Koehler et al.[4] were adjusted to fit experimental data of the total cross section. The total cross section above 7 MeV was evaluated with spline fitting of experimental data. For TNG calculation, the optical model parameters and the level denisty parameters were adjusted to reproduce experimental data of (n,p), (n,α) reactions and elastic scattering. Direct inelastic processes for five excited levels (Q = -2.12, -4.45, -5.02, -6.74 and -6.79 MeV) were considered with DWBA calculation. The capture cross section was calculated from MLBW formula by adopting resonance parameters recommended by Mughabghab et al.[5].

Fig. 1 and Fig. 2 show angular distributions of elastically scattered neutrons and the results of evaluation for total cross section, respectively. The comparison with DDX data of Tohoku University[6] is shown in Fig. 3. The results of this work are in good agreement with the experimental data. They were compiled in the ENDF/B-V format.

References:

1) Komada, S. et al.; private communication.

2) Fu, C.Y.; ORNL/TM-7042 (1980).

3) Shibata, K. and Fu, C.Y.; ORNL/TM-10093 (1986).

4) Koehler, P.E., Knox, H.D., Resler, D.A., Lane, R.O., and Millener, D.J.; Nulc. Phys., A394, 221 (1983).

5) Mughabghab, S.F., Divadeenam, M. and Holden, N.E.; Neutron Cross Section, Vol. 1 (1981).

6) Baba, M. et al.; Proc. Int. Conf. on Nuclear Data for Basic and Applied Science, 1985 Santa Fe, p.223.

7) Lane, R.O. et al.; Phys. Rev., C2, 2097 (1970).

8) Nelson, C.E., et al.; Nucl. Phys., A217, 546 (1973).

Table 1 The Evaluated Quantities

reactions	cross section	angular distribution of secondary neutron	energy spectrum of secondary neutron	energy range of incident neutron
total	O	–	–	10^{-5}eV-20MeV
elastic	O	O	–	10^{-5}eV-20MeV
inelastic	O	O	O	2.3 -20MeV
capture	O	–	–	10^{-5}eV-20MeV
(n,2n)	O	O	O	12.5 -20MeV
(n,p)	O	–	–	11.7 -20MeV
(n,α)	O	–	–	7.2 -20MeV
(n,np)	O	O	O	12.3 -20MeV
(n,nα)	O	O	O	9.5 -20MeV

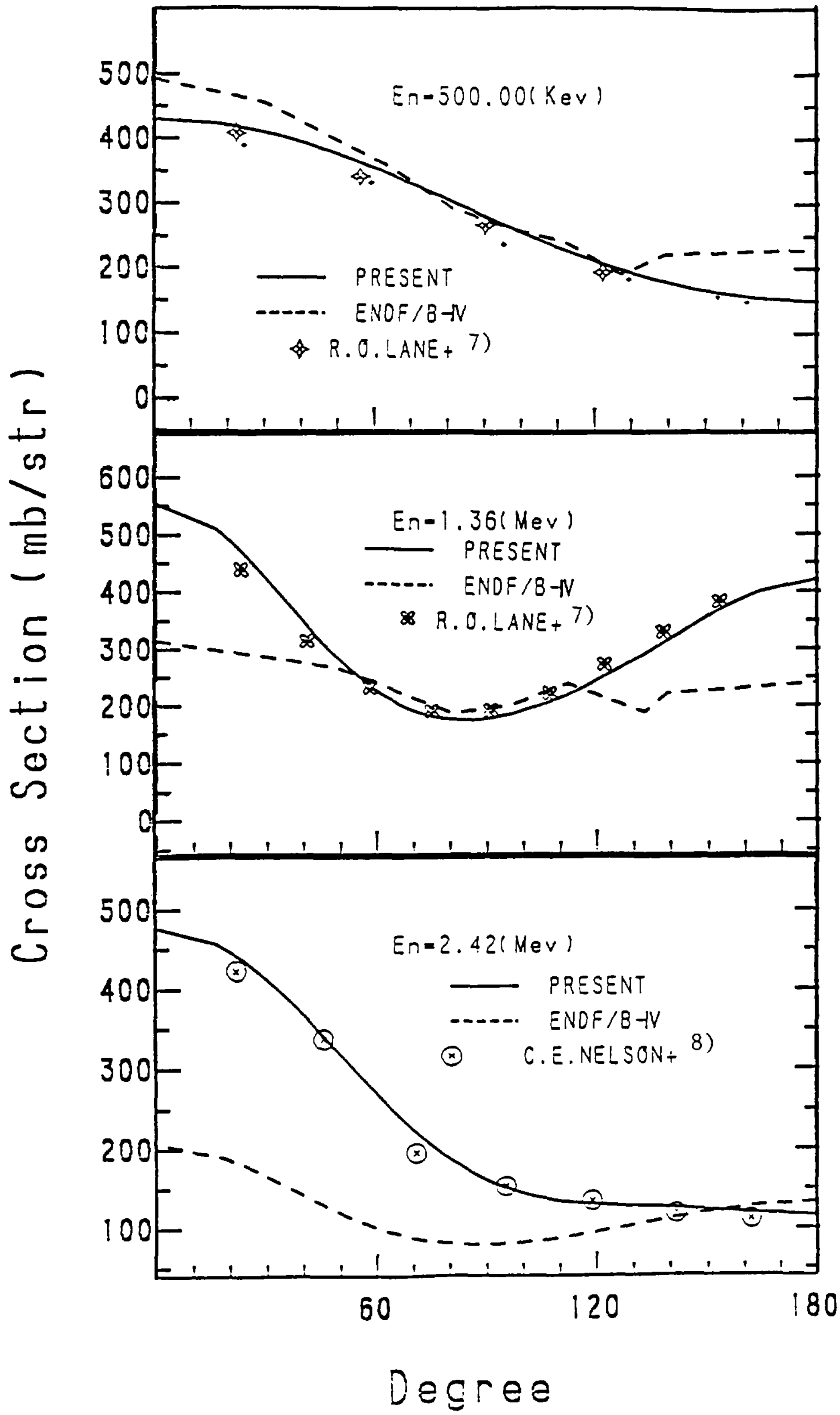

Fig. 1 The Angular Distributions of Elastically scattered neutrons.

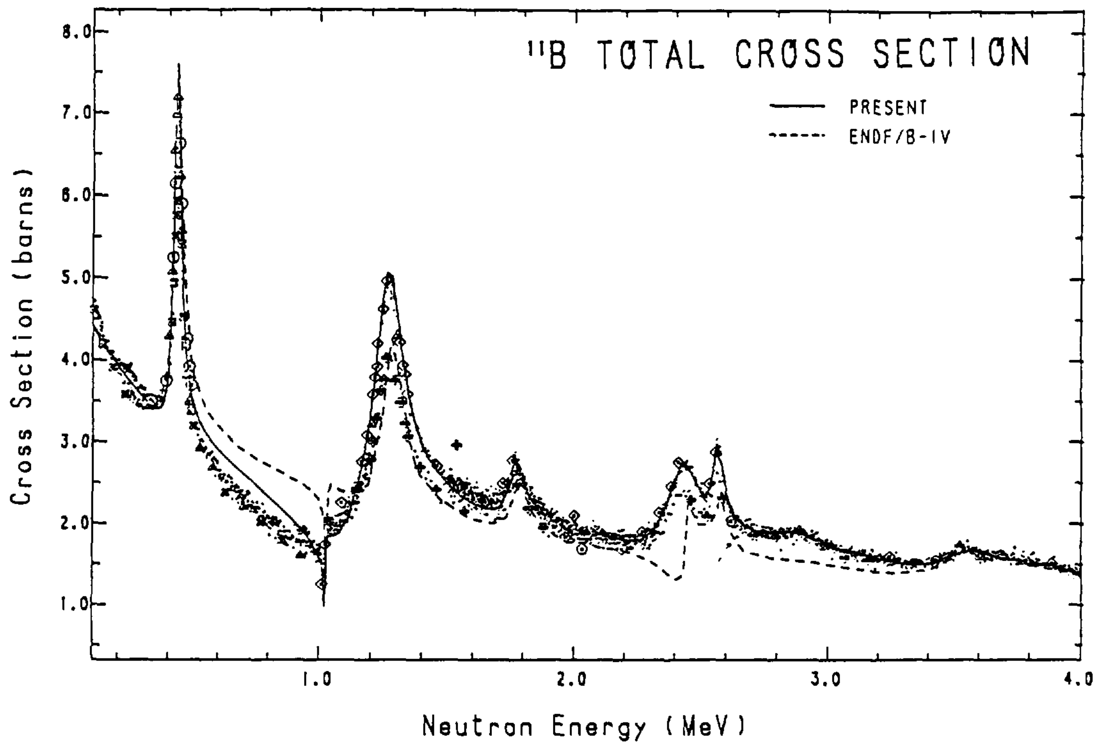

Fig. 2 Total Cross Section.

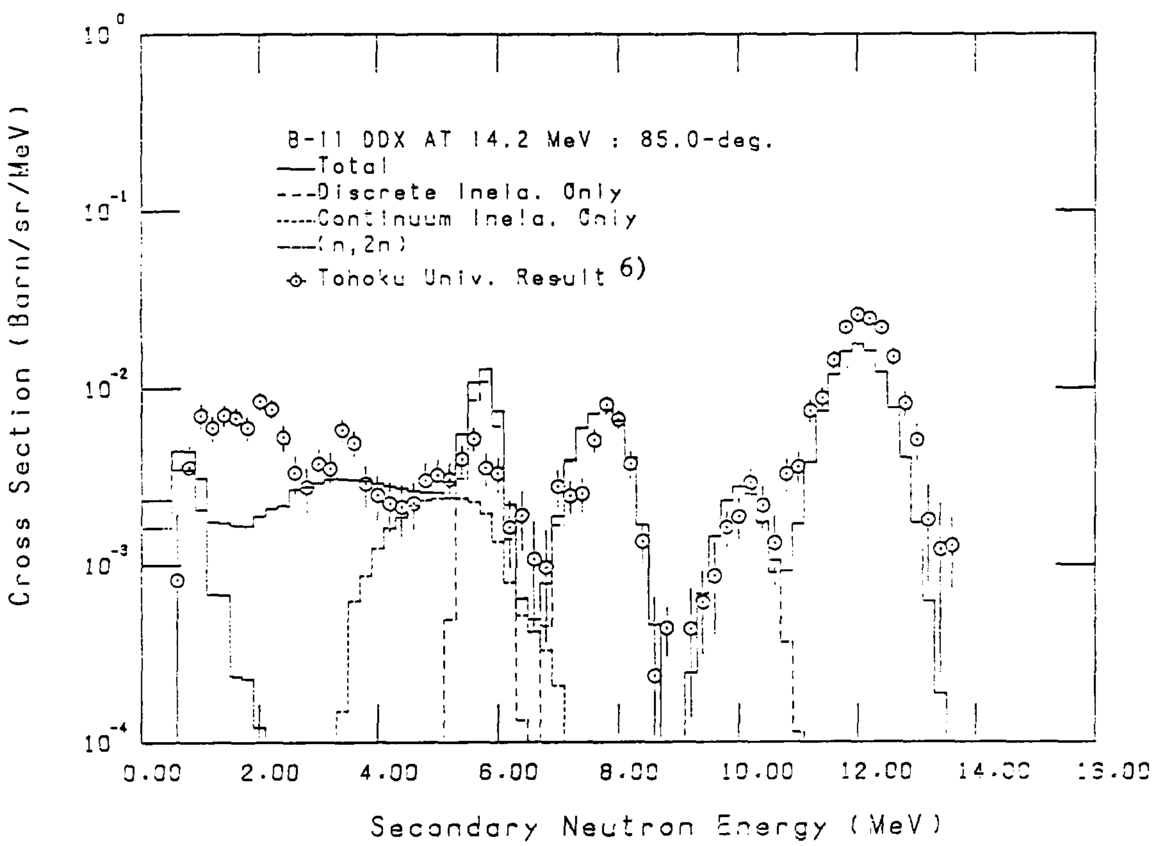

Fig. 3 Comparison of present result and measured DDX data.

II-C-4

Evaluation of Neutron Nuclear Data for Natural Silver and its Isotopes

LIU Ting jin,* Tsuneo NAKAGAWA and Keiichi SHIBATA

Neutron nuclear data of natural silver and its isotopes (^{107}Ag and ^{109}Ag) have been evaluated in the energy range from 10^{-5} eV to 20 MeV. The evaluated quantities are the total, elastic and inelastic scattering, radiative capture, γ-ray production, (n,2n), (n,3n), (n,p), (n,α), (n,np), and (n,nα) reaction cross sections, the resonance parameters and the angular and energy distributions of emitted neutrons and γ-rays.

Above 100 keV, the cross sections were calculated with the multi-step statistical model using the TNG code[1]. The precompound mode was taken into account in the calculations. The parameters of the neutron optical potential obtained by Smith et al.[2] were slightly modified and used throughout this work.

Figures 1 and 2 show the evaluated capture cross sections. In these figures, the enhancement seen above 10 MeV comes from the precompound capture. The inelastic scattering cross sections of ^{107}Ag are illustrated in Fig. 3.

References:

1) Fu, C.Y. : ORNL/TM-7042 (1980).

2) Smith, A.B., et al. : Nucl. Phys., A415, 1 (1984).

3) Nishimura, K., et al. : Nucl. Phys., 70, 421 (1965).

4) Smith, A., et al. : Nucl. Phys., A332, 297 (1979).

---

* On leave from the Institute of Atomic Energy, China

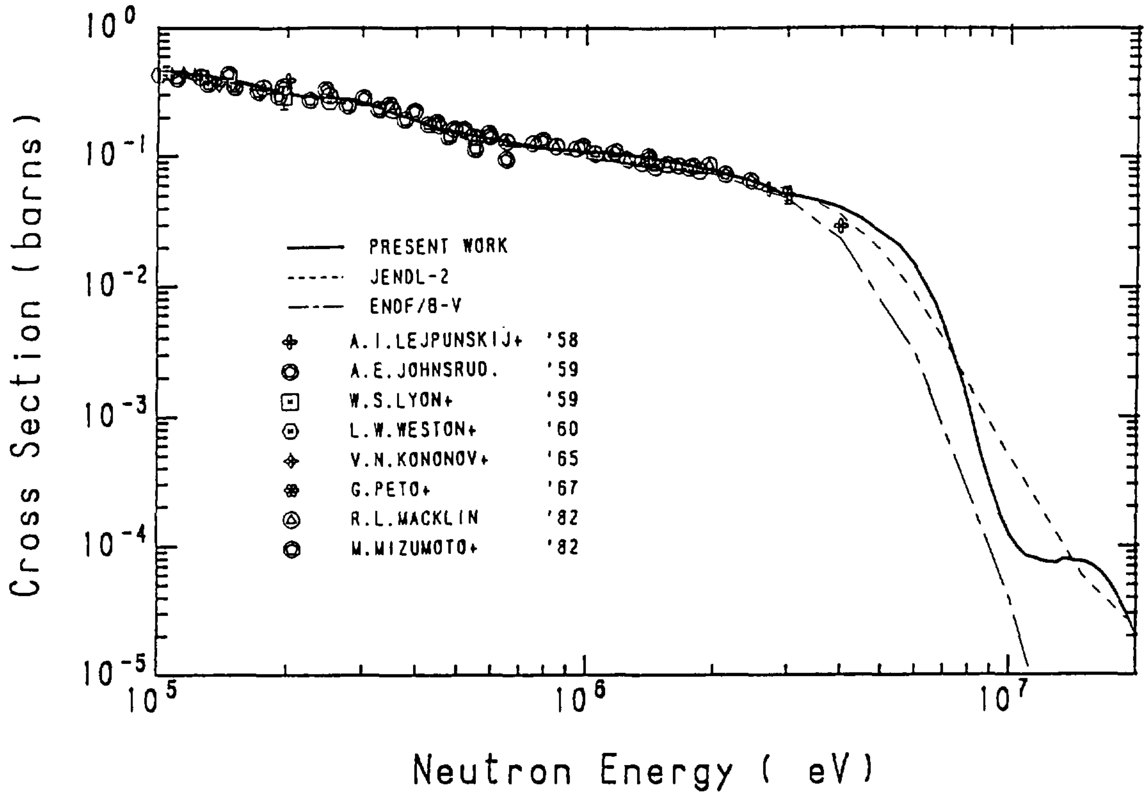

Fig. 1 Capture cross sections of ^{107}Ag.

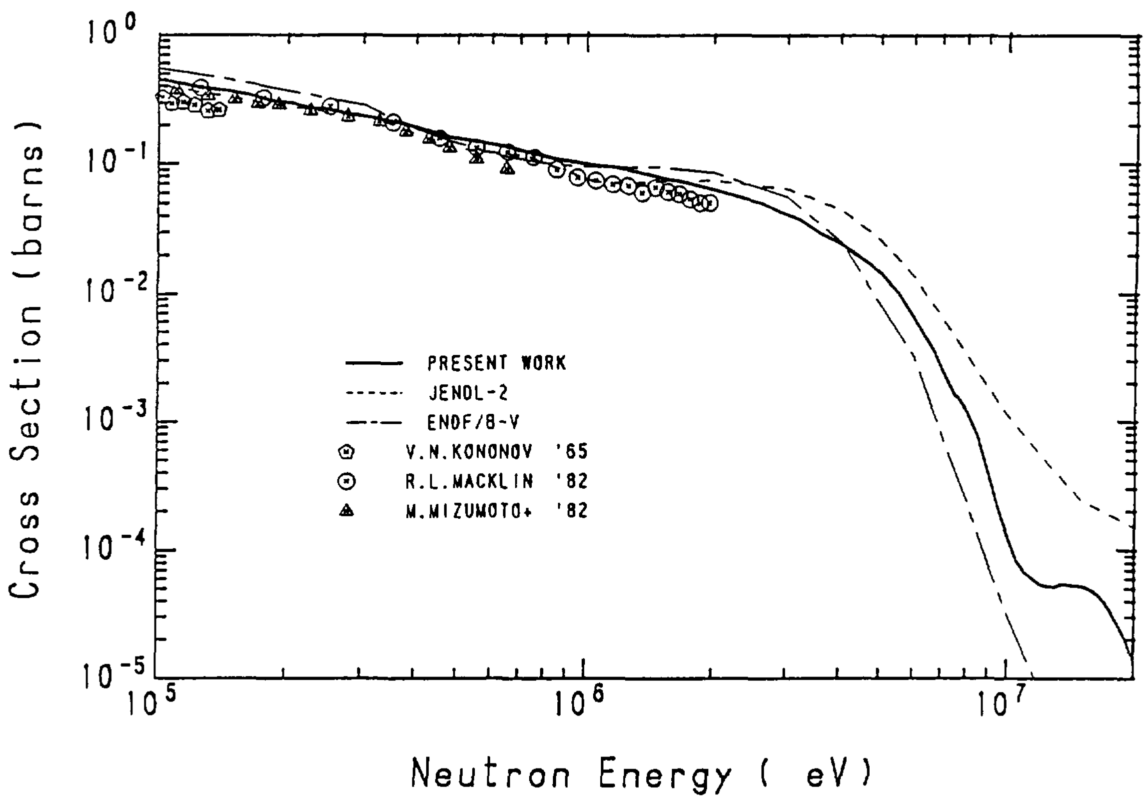

Fig. 2 Capture cross sections of ^{109}Ag.

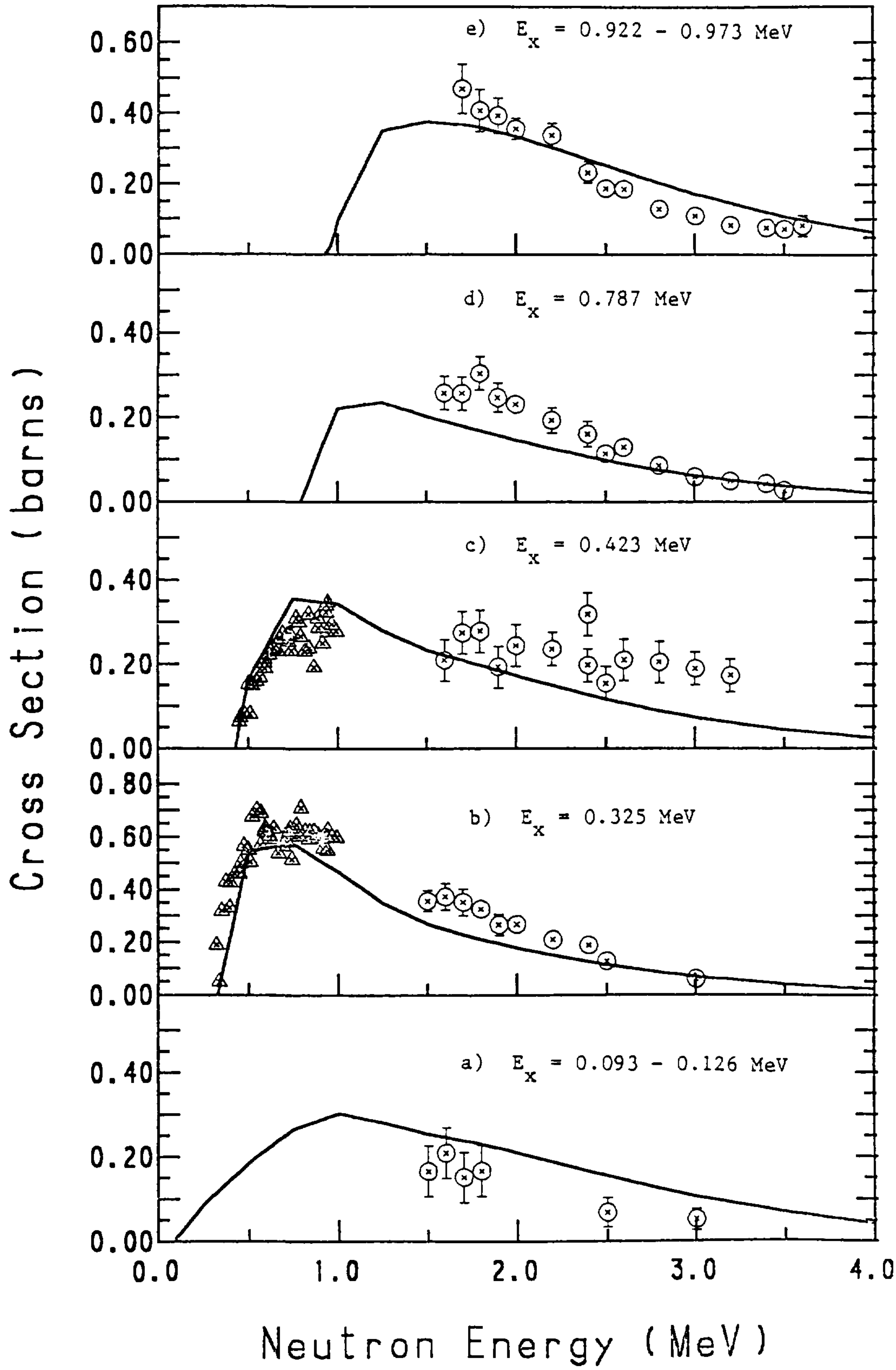

Fig. 3 Inelastic scattering cross sections of ^{107}Ag.
Data symbols denote : solid line = present work, triangles = ref. 3 and circles = ref. 4.

II-C-5

Evaluation of Neutron Nuclear Data for ^{252}Cf and ^{250}Bk

Tsuneo NAKAGAWA

Neutron nuclear data of ^{252}Cf and ^{250}Bk have been evaluated in the energy range from 10^{-5} eV to 20 MeV. The cross sections evaluated in this work are the total, elastic and inelastic scattering, (n,2n), (n,3n) and (n,4n), fission and capture cross sections. Angular and energy distributions of emitted neutrons were also evaluated. The present evaluation was based on systematics of the data of neighboring nuclides, optical and statistical model calculations. For the both nuclides, cross sections below 30 keV were represented with resolved and unresolved resonance parameters. The resolved resonance parameters of ^{252}Cf were evaluated below 1 keV on the bases of experimental data. In the case of ^{250}Bk, hypothetical resolved resonances were given below 100 eV. The results are very consistent with existing experimental data of ^{252}Cf fission cross section and thermal cross sections. A paper on this subject will be submitted to JAERI-M report.

II-C-6

Compilation of JENDL-3

Nuclear Data Center

The compilatioan of JENDL-3 have been finished for the most part and the benchmark tests for major nuclides are in progress. The data file for these tests was named JENDL-3T temporarily. The outlines and some features of JENDL-3 have been described elsewhere[1].

Table 1 shows the nuclides which are stored in a general purpose file of JENDL-3, and Table 2 also shows the fission-product nuclides in JENDL-3.

In JENDL-3, photon-production data are newly adopted for major nuclides or elements, as shown in Table 1, and the JENDL-2 data on high-energy neutrons are sharply revised for almost all of the nuclides, in considering wide uses in development of fusion reactors.

The data evaluation was made by thirty-odd evaluators and several working groups in JNDC. The compilation for the evaluated data was made by the compilation group in Nuclear Data Center of JAERI.

After the JENDL-3T data are modified on the basis of the results of the benchmark tests, JENDL-3 will be open in the next year.

Reference:

1) T. Asami: Proc. of the 1986 Seminar on Nuclear Data, JAERI-M 87-025 (1987) p.1.

Table 1. Nuclides in the General Purpose File of JENDL-3.
The underlines denote the nuclides stored newly in JENDL-3. The asterisks show the nuclides with the evaluated data for photon Production.

Z	Nuclide	Z	Nuclide	Z	Nuclide
1	*^{1}H, ^{2}H	21	^{45}Sc	63	*$\underline{\mathrm{Eu}}$, ^{151}Eu, ^{153}Eu
2	$\underline{^{3}\mathrm{He}}$, $\underline{^{4}\mathrm{He}}$	22	*$\underline{\mathrm{Ti}}$, $\underline{^{40}\mathrm{Ti}}$, $\underline{^{47}\mathrm{Ti}}$, $\underline{^{48}\mathrm{Ti}}$, $\underline{^{49}\mathrm{Ti}}$, $\underline{^{50}\mathrm{Ti}}$		
3	*^{6}Li, *^{7}Li	23	^{51}V	72	*$\underline{\mathrm{Hf}}$, ^{174}Hf, ^{176}Hf, ^{177}Hf, ^{178}Hf,
4	*^{9}Be	24	*Cr, ^{50}Cr, ^{52}Cr, ^{53}Cr, ^{54}Cr		^{179}Hf, ^{180}Hf
5	^{10}B, $\underline{^{11}\mathrm{B}}$	25	*^{55}Mn	73	*^{181}Ta
6	*^{12}C	26	*Fe, ^{54}Fe, ^{56}Fe, ^{57}Fe, ^{58}Fe	74	*$\underline{\mathrm{W}}$, $\underline{^{180}\mathrm{W}}$, $\underline{^{182}\mathrm{W}}$, $\underline{^{183}\mathrm{W}}$, $\underline{^{184}\mathrm{W}}$, $\underline{^{186}\mathrm{W}}$
7	*$\underline{^{14}\mathrm{N}}$	27	^{59}Co	82	*Pb, ^{204}Pb, ^{206}Pb, ^{207}Pb, ^{208}Pb
8	*$\underline{^{16}\mathrm{O}}$	28	*Ni, ^{58}Ni, ($\underline{^{59}\mathrm{Ni}}$), ^{60}Ni, ^{61}Ni, ^{62}Ni,	83	*$\underline{^{209}\mathrm{Bi}}$
9	^{19}F		^{64}Ni	90	^{228}Th, ^{230}Th, ^{232}Th, ^{233}Th,
11	*^{23}Na	29	*Cu, ^{63}Cu, ^{65}Cu		^{234}Th
12	*$\underline{\mathrm{Mg}}$, $\underline{^{24}\mathrm{Mg}}$, $\underline{^{25}\mathrm{Mg}}$, $\underline{^{26}\mathrm{Mg}}$	40	$\underline{\mathrm{Zr}}$, ^{90}Zr, ^{91}Zr, ^{92}Zr, ^{94}Zr, ^{96}Zr	91	$\underline{^{231}\mathrm{Pa}}$, ^{233}Pa
13	*^{27}Al			92	$\underline{^{232}\mathrm{U}}$, ^{233}U, ^{234}U, *^{235}U, ^{236}U, *^{238}U
14	*Si, $\underline{^{28}\mathrm{Si}}$, $\underline{^{29}\mathrm{Si}}$, $\underline{^{30}\mathrm{Si}}$	41	*^{93}Nb, ($\underline{^{94}\mathrm{Nb}}$)	93	^{237}Np, ^{239}Np
15	$\underline{^{31}\mathrm{P}}$	42	*Mo, ^{92}Mo, ^{94}Mo, ^{95}Mo, ^{96}Mo, ^{97}Mo,	94	^{236}Pu, ^{238}Pu, *^{239}Pu, ^{240}Pu, ^{241}Pu,
16	$\underline{\mathrm{S}}$, $\underline{^{32}\mathrm{S}}$, $\underline{^{33}\mathrm{S}}$, $\underline{^{34}\mathrm{S}}$, $\underline{^{36}\mathrm{S}}$		^{98}Mo, ^{100}Mo		^{242}Pu
17	$\underline{\mathrm{Cl}}$, $\underline{^{35}\mathrm{Cl}}$, $\underline{^{37}\mathrm{Cl}}$			95	^{241}Am, ^{242g}Am, ^{242m}Am, ^{243}Am
18	$\underline{^{40}\mathrm{Ar}}$	47	*$\underline{\mathrm{Ag}}$, ^{107}Ag, ^{109}Ag	96	^{242}Cm, ^{243}Cm, ^{244}Cm, ^{245}Cm, $\underline{^{246}\mathrm{Cm}}$,
19	$\underline{\mathrm{K}}$, $\underline{^{39}\mathrm{K}}$, $\underline{^{40}\mathrm{K}}$, $\underline{^{41}\mathrm{K}}$	48	$\underline{\mathrm{Cd}}$		$\underline{^{247}\mathrm{Cm}}$, $\underline{^{248}\mathrm{Cm}}$, $\underline{^{249}\mathrm{Cm}}$
20	*Ca, ^{40}Ca, ^{42}Ca, ^{43}Ca, ^{44}Ca			97	$\underline{^{249}\mathrm{Bk}}$, $\underline{^{250}\mathrm{Bk}}$
	^{46}Ca, ^{48}Ca	51	$\underline{\mathrm{Sb}}$, ^{121}Sb, ^{123}Sb	98	$\underline{^{249}\mathrm{Cf}}$, $\underline{^{250}\mathrm{Cf}}$, $\underline{^{251}\mathrm{Cf}}$, $\underline{^{252}\mathrm{Cf}}$

Table 2. Fission Product Nuclides in JENDL-3.
The underlines denote the nuclides stored newly in JENDL-3.

Z	Nuclide
33	$\underline{^{75}\mathrm{As}}$
34	$\underline{^{74}\mathrm{Se}}$, $\underline{^{76}\mathrm{Se}}$, $\underline{^{77}\mathrm{Se}}$, $\underline{^{78}\mathrm{Se}}$, $\underline{^{79}\mathrm{Se}}$, $\underline{^{80}\mathrm{Se}}$, $\underline{^{82}\mathrm{Se}}$
35	$\underline{^{79}\mathrm{Br}}$, $\underline{^{81}\mathrm{Br}}$
36	$\underline{^{78}\mathrm{Kr}}$, $\underline{^{80}\mathrm{Kr}}$, $\underline{^{82}\mathrm{Kr}}$, $^{83}\mathrm{Kr}$, $^{84}\mathrm{Kr}$, $^{85}\mathrm{Kr}$, $^{86}\mathrm{Kr}$
37	$^{85}\mathrm{Rb}$, $^{87}\mathrm{Rb}$
38	$^{86}\mathrm{Sr}$, $^{87}\mathrm{Sr}$, $^{88}\mathrm{Sr}$, $\underline{^{89}\mathrm{Sr}}$, $^{90}\mathrm{Sr}$
39	$^{89}\mathrm{Y}$, $\underline{^{91}\mathrm{Y}}$
40	$^{90}\mathrm{Zr}$, $^{91}\mathrm{Zr}$, $^{92}\mathrm{Zr}$, $^{93}\mathrm{Zr}$, $^{94}\mathrm{Zr}$, $^{95}\mathrm{Zr}$, $^{96}\mathrm{Zr}$
41	$^{93}\mathrm{Nb}$, $\underline{^{94}\mathrm{Nb}}$, $\underline{^{95}\mathrm{Nb}}$
42	$^{92}\mathrm{Mo}$, $^{94}\mathrm{Mo}$, $^{95}\mathrm{Mo}$, $^{96}\mathrm{Mo}$, $^{97}\mathrm{Mo}$, $^{98}\mathrm{Mo}$, $\underline{^{99}\mathrm{Mo}}$, $^{100}\mathrm{Mo}$
43	$^{99}\mathrm{Tc}$
44	$\underline{^{96}\mathrm{Ru}}$, $\underline{^{98}\mathrm{Ru}}$, $\underline{^{99}\mathrm{Ru}}$, $^{100}\mathrm{Ru}$, $^{101}\mathrm{Ru}$, $^{102}\mathrm{Ru}$, $^{103}\mathrm{Ru}$, $^{104}\mathrm{Ru}$, $^{106}\mathrm{Ru}$
45	$^{103}\mathrm{Rh}$, $\underline{^{105}\mathrm{Rh}}$
46	$\underline{^{102}\mathrm{Pd}}$, $^{104}\mathrm{Pd}$, $^{105}\mathrm{Pd}$, $^{106}\mathrm{Pd}$, $^{107}\mathrm{Pd}$, $^{108}\mathrm{Pd}$, $^{110}\mathrm{Pd}$
47	$^{107}\mathrm{Ag}$, $^{109}\mathrm{Ag}$, $\underline{^{110m}\mathrm{Ag}}$
48	$\underline{^{106}\mathrm{Cd}}$, $\underline{^{108}\mathrm{Cd}}$, $^{110}\mathrm{Cd}$, $^{111}\mathrm{Cd}$, $^{112}\mathrm{Cd}$, $^{113}\mathrm{Cd}$, $^{114}\mathrm{Cd}$, $^{116}\mathrm{Cd}$
49	$\underline{^{113}\mathrm{In}}$, $^{115}\mathrm{In}$
50	$\underline{^{112}\mathrm{Sn}}$, $\underline{^{114}\mathrm{Sn}}$, $\underline{^{115}\mathrm{Sn}}$, $\underline{^{116}\mathrm{Sn}}$, $\underline{^{117}\mathrm{Sn}}$, $\underline{^{118}\mathrm{Sn}}$, $\underline{^{119}\mathrm{Sn}}$, $\underline{^{120}\mathrm{Sn}}$, $\underline{^{122}\mathrm{Sn}}$, $\underline{^{123}\mathrm{Sn}}$, $\underline{^{124}\mathrm{Sn}}$, $\underline{^{126}\mathrm{Sn}}$
51	$^{121}\mathrm{Sb}$, $^{123}\mathrm{Sb}$, $^{124}\mathrm{Sb}$, $\underline{^{125}\mathrm{Sb}}$
52	$\underline{^{120}\mathrm{Te}}$, $\underline{^{122}\mathrm{Te}}$, $\underline{^{123}\mathrm{Te}}$, $\underline{^{124}\mathrm{Te}}$, $\underline{^{125}\mathrm{Te}}$, $\underline{^{126}\mathrm{Te}}$, $\underline{^{127m}\mathrm{Te}}$, $^{128}\mathrm{Te}$, $\underline{^{129m}\mathrm{Te}}$, $\underline{^{130}\mathrm{Te}}$
53	$^{127}\mathrm{I}$, $^{129}\mathrm{I}$, $\underline{^{131}\mathrm{I}}$
54	$\underline{^{124}\mathrm{Xe}}$, $\underline{^{126}\mathrm{Xe}}$, $\underline{^{128}\mathrm{Xe}}$, $\underline{^{129}\mathrm{Xe}}$, $\underline{^{130}\mathrm{Xe}}$, $^{131}\mathrm{Xe}$, $^{132}\mathrm{Xe}$, $^{133}\mathrm{Xe}$, $^{134}\mathrm{Xe}$, $^{135}\mathrm{Xe}$, $^{136}\mathrm{Xe}$
55	$^{133}\mathrm{Cs}$, $\underline{^{134}\mathrm{Cs}}$, $^{135}\mathrm{Cs}$, $\underline{^{136}\mathrm{Cs}}$, $^{137}\mathrm{Cs}$
56	$\underline{^{130}\mathrm{Ba}}$, $\underline{^{132}\mathrm{Ba}}$, $^{134}\mathrm{Ba}$, $^{135}\mathrm{Ba}$, $^{136}\mathrm{Ba}$, $^{137}\mathrm{Ba}$, $^{138}\mathrm{Ba}$, $\underline{^{140}\mathrm{Ba}}$
57	$\underline{^{138}\mathrm{La}}$, $^{139}\mathrm{La}$
58	$^{140}\mathrm{Ce}$, $\underline{^{141}\mathrm{Ce}}$, $^{142}\mathrm{Ce}$, $^{144}\mathrm{Ce}$
59	$^{141}\mathrm{Pr}$, $\underline{^{143}\mathrm{Pr}}$
60	$^{142}\mathrm{Nd}$, $^{143}\mathrm{Nd}$, $^{144}\mathrm{Nd}$, $^{145}\mathrm{Nd}$, $^{146}\mathrm{Nd}$, $\underline{^{147}\mathrm{Nd}}$, $^{148}\mathrm{Nd}$, $^{150}\mathrm{Nd}$
61	$^{147}\mathrm{Pm}$, $\underline{^{148g}\mathrm{Pm}}$, $\underline{^{148m}\mathrm{Pm}}$, $\underline{^{149}\mathrm{Pm}}$
62	$\underline{^{144}\mathrm{Sm}}$, $^{147}\mathrm{Sm}$, $^{148}\mathrm{Sm}$, $^{149}\mathrm{Sm}$, $^{150}\mathrm{Sm}$, $^{151}\mathrm{Sm}$, $^{152}\mathrm{Sm}$, $\underline{^{153}\mathrm{Sm}}$, $^{154}\mathrm{Sm}$
63	$^{151}\mathrm{Eu}$, $^{152}\mathrm{Eu}$, $^{153}\mathrm{Eu}$, $^{154}\mathrm{Eu}$, $^{155}\mathrm{Eu}$, $\underline{^{156}\mathrm{Eu}}$
64	$\underline{^{152}\mathrm{Gd}}$, $\underline{^{154}\mathrm{Gd}}$, $^{155}\mathrm{Gd}$, $^{156}\mathrm{Gd}$, $^{157}\mathrm{Gd}$, $^{158}\mathrm{Gd}$, $^{160}\mathrm{Gd}$
65	$^{159}\mathrm{Tb}$

II-C-7

Evaluation of Neutron Cross Sections of Fission Products for JENDL-3

JNDC Subworking Group on Fission Product Nuclear Data

Evaluation work on neutron cross sections of fission product nuclides is in progress for JENDL-3. Compared to JENDL-2, the number of FP nuclides is extended to 172 by adding As, Se, Br, Sn and Te isotopes, and some short-lived nuclides. Threshold reaction cross sections are also newly contained in the scope for general applications.

Resonance parameters and nuclear model parameters, for calculating neutron cross sections with spherical optical model and statistical theory, were evaluated for the new nuclides of JENDL-3. The (n,2n), (n,p), (n,α), (n,np) and (n,nα) cross sections were preliminarily evaluated for all FP nuclides by using the multi-step evaporation and preequilibrium model calculation code, PEGASUS[(1)]. The Kalbach's constant K, which represents the strength of the preequilibrium transition rate, was estimated as $K \simeq 0.1/(g/A)^3$, where g is the single particle level density.

Figure 1 shows the experiment-to-calculation ratios of 14.5 MeV (n,2n) and (n,p) cross sections. The (n,2n) cross sections are predicted fairly well. The (n,p) cross sections are on the average a factor of 2 $\sim$ 3 underestimated. The same is true for (n,α) cross sections. The calculations are normalized to the experimental data or to the 14.5 MeV systematics in the final results. In Fig. 2 are shown the (n,2n) excitation cross sections of even Nd isotopes in comparions with experimental data.

Integral test is made using JAERI-FAST type 70-group cross sections with resonance self-shielding factors, and the neutron spectrum data for STEK, CFRMF and EBR-II. Covariances of flux and cross sections are considered. Code system for integral test, containing calculation of covarince matrices and cross section adjustment based on integral data, was developed. Group cross sections for JENDL-2 FP nuclides were generated. Preliminary results of the integral test of JENDL-2 FP cross sections are obtained. The results are being taken into account in the evaluation of capture and inelastic scattering cross sections for JENDL-3.

Reference:

1) S. Iijima, T. Sugi, T. Nakagawa and T. Nishigori, to be published in JAERI-M report.

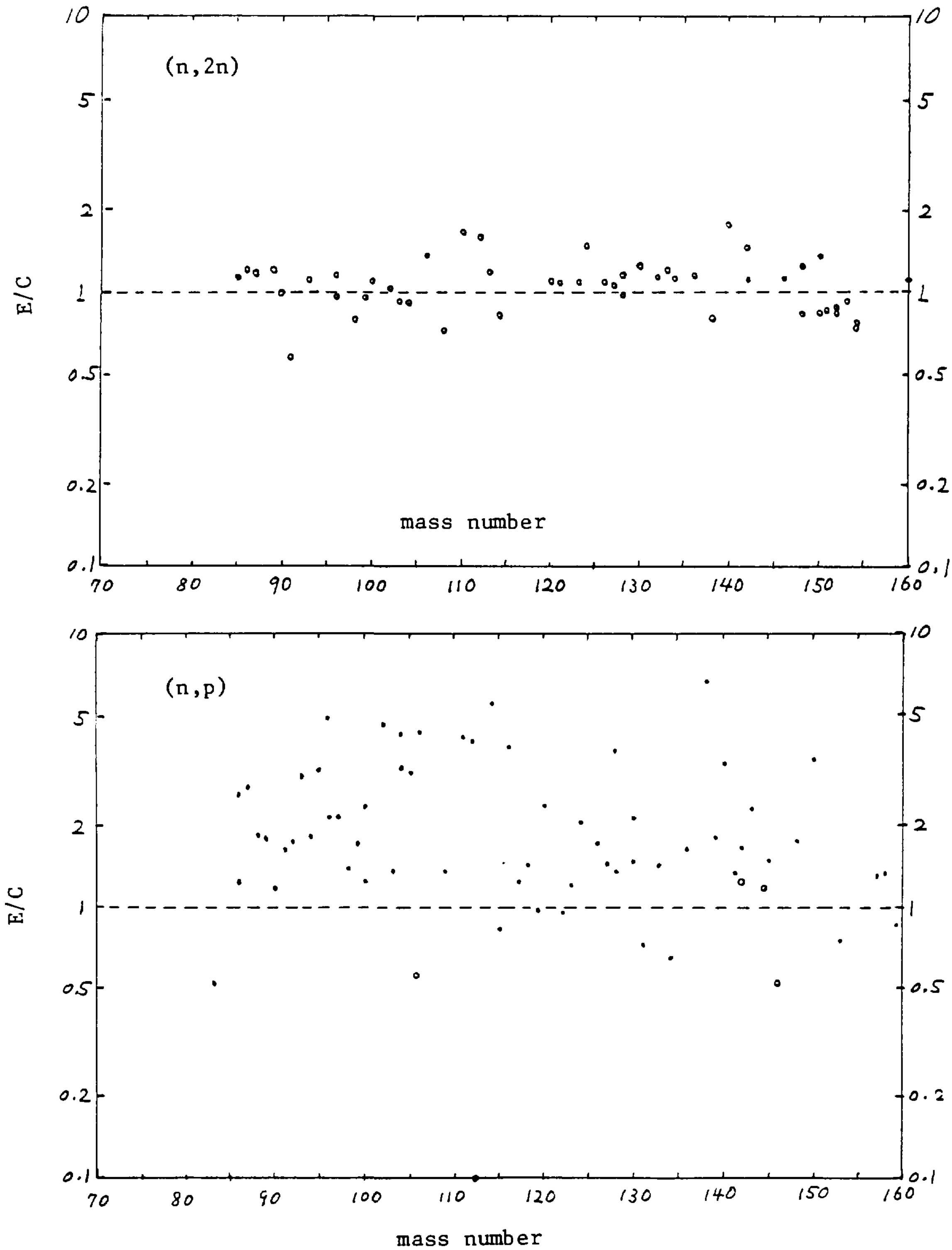

Fig. 1 Experiment-to-calculation ratios of (n,2n) and (n,p) cross sections at 14.5 MeV

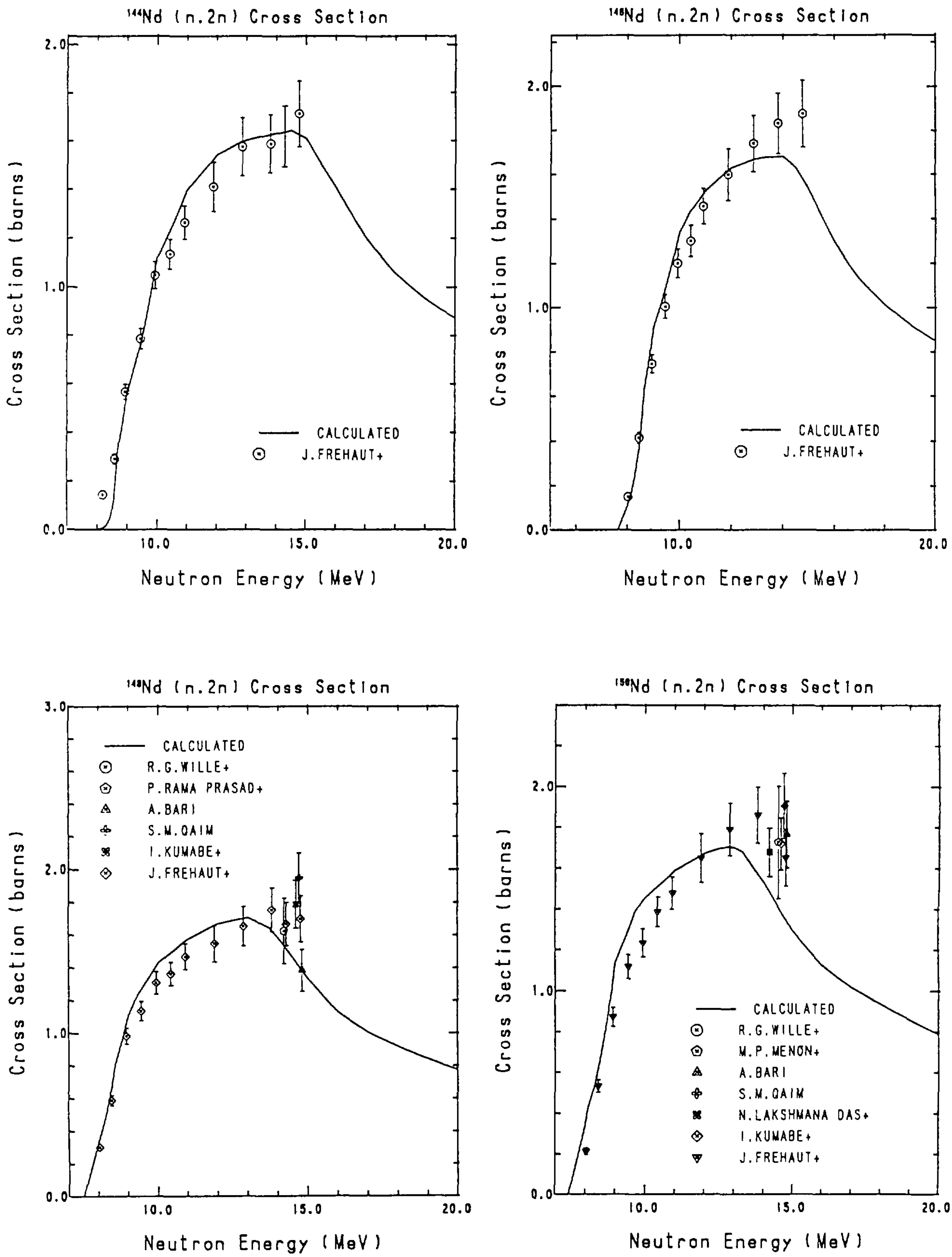

Fig. 2 (n,2n) reaction cross sections of Neodymium even mass isotopes

II-C-8 Evaluation of Heavy Nuclide Data for JENDL-3

JNDC Subworking Group on Heavy Nuclide Data

Evaluation work has been completed for 21 nuclides; ^{228}Th, ^{230}Th, ^{232}Th, ^{233}Th, ^{234}Th, ^{231}Pa, ^{233}Pa, ^{232}U, ^{233}U, ^{234}U, ^{235}U, ^{236}U, ^{238}U, ^{237}Np, ^{239}Np, ^{236}Pu, ^{238}Pu, ^{239}Pu, ^{240}Pu, ^{241}Pu and ^{242}Pu. Among them, ^{231}Pa and ^{233}U are newly added nuclides to JENDL. JENDL-2 data of minar isotopes such as ^{228}Th, ^{230}Th, ^{234}Th and ^{239}Np were adopted without any modification.

Fission cross sections of ^{235}U, ^{238}U, ^{239}Pu, ^{240}Pu and ^{241}Pu and neutron capture cross section of ^{238}U were evaluated in the energy range above 50 keV with simultaneous evaluation method[1)] based on generalized least-squares fitting and second order B-spline functions. Almost all experimental data reported after 1970 were taken into account. Their covariance matrixes were constructed from reported information on error.

An example of the evaluation is shown in Fig. 1. The present evaluation is in very good agreement with experimental data. However, below 1 MeV, the fission cross sections of ^{235}U and ^{239}Pu are few percents lower than JENDL-2.

The inelastic scattering cross sections were modified from JENDL-2 by coupled-channel or DWBA calculations. In many cases, new results are larger than JENDL-2.

Resonance parameters were also improved for almost all nuclides. Those of ^{232}Th were replaced with new experimental results by Kobayashi et al.[2)] In the case of ^{238}U, resolved resonance region was extended up to 9.5 keV on the basis of Olsen's new analysis[3)]. For ^{239}Pu, Reich-Moore parameters obtained by Derrien et al.[4] were tentatively adopted. Unresolved resonance parameters were determined to reproduce the evaluated cross sections.

Fission spectra of major isotopes were calculated from Madland-Nix formula by adopting parameters evaluated by Madland and Nix[5]. Delayed neutron spectra recommended by Saphier et al.[6] were widely adopted. Neutron spectra of other reactions were calculated with a precompound and multistep evaporation code PEGASUS[7].

For ^{235}U, ^{238}U and ^{239}Pu, gamma-ray production data were evaluated with GNASH code[8].

Neutron nuclear data of heavy nuclides have been modified from JENDL-2 more or less. Benchmark test of the evaluated data is in progress. Before release of JENDL-3, re-investigation of important data might be needed if problems will be found by the benchmark test.

References:

1) Y. Kanda, et al.: Proc. of the International Conf. on Nucl. data for Basic and Applied Science, Santa Fe (1985), Vol.2, 1567 (1986).

2) K. Kobayashi, et al.: private communication to evaluator. (1985).

3) D.K. Olsen: Nucl. Sci. Eng., 94, 102 (1986).

4) H. Derrien, et al.: ORNL/TM-10098 (1986).

5) D.G. Madland and J.R. Nix: Nucl. Sci. Eng., 81, 213 (1982).

6) D. Saphier, et al.: Nucl. Sci. Eng., 62, 660 (1977).

7) S. Iijima, et al.: JAERI-M 87-025, p.337 (1987).

8) P.G. Young and E.D. Arthur: LA-6947 (1978).

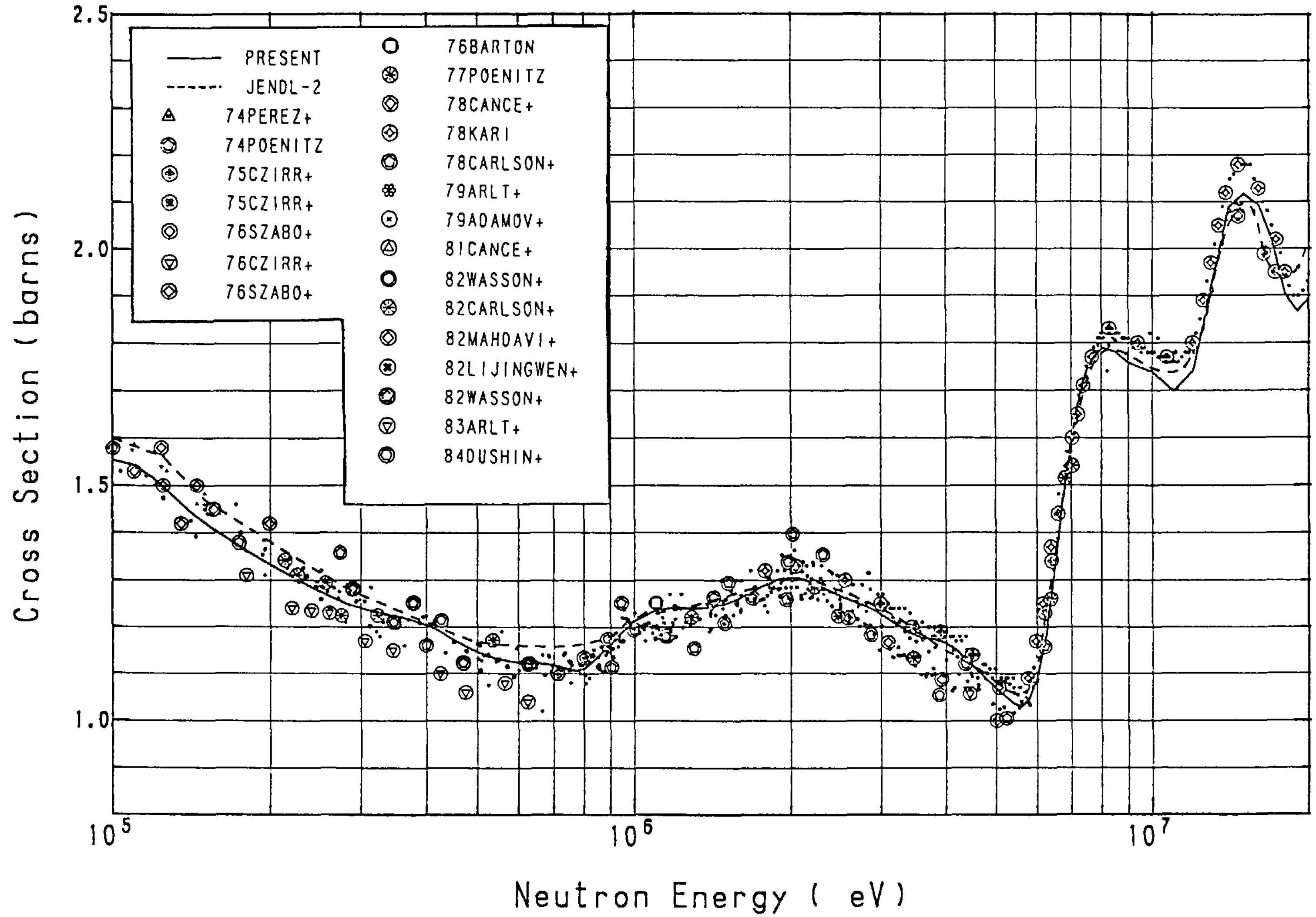

Fig. 1 Fission cross section of ^{235}U

III. Kinki University

Department of Reactor Engineering

III-1

Predictions of the (n,2n) Cross Sections Averaged Over the U-235 and Cf-252 Fission Neutron Spectra for Light Nuclei

O. Horibe

1. Basis of the predictions

We already found the empirical rule[1] for the (n,p) and (n,α) cross sections. For the (n,2n), we also assumed the similar type of formula for the predictions including a slight change of meaning of E_T from E_{eff} defined by Hughes[2], as follows.

$$\log(25\bar{\sigma} A^{-2/3} E_T^{-1/2}) = \alpha(t) E_T + \beta, \qquad (1)$$

where $\bar{\sigma}$ is the averaged cross section, A, the mass number of target nucleus, E_T, reaction threshold energy, α, a constant dependent on t which is neutron-excess number of target nucleus and β, normalization constant.

2. Data used for the predictions

We used the data evaluated by Calamand[3] for the U-235 spectrum averaged cross sections, denoted by $\bar{\sigma}$(U) and also by Mannhart[4] for the Cf-252 spectrum averaged ones, denoted by $\bar{\sigma}$(Cf). The number of these data available for $t \leq 2$ is so small that we calculated $\bar{\sigma}$(U) and

$\bar{\sigma}$(Cf) using measured values of the monochromatic neutron cross sections[5] and also spectra of the U-235 and Cf-252 fission neutrons, of which shapes assumed are as follows, respectively.

$$\chi(E)=0.4303E^{1/2}\ \exp(-E/0.998)\sinh(2.249E)^{1/2}, \quad (1)$$

and

$$\chi(E)=0.6672E^{1/2}\exp(-1.5E/2.13). \quad \text{(Maxwellian)}$$

Fig. 1 shows plots of $\bar{\sigma}(Cf)/\bar{\sigma}(U)$ in log. scale agaist E_T. Values of E_T were quoted from those by Calmand[3]. A line indicated by (1) is the best fit line to the data points for the calculated $\bar{\sigma}$(U) and $\bar{\sigma}$(Cf) and also the measured values of ^{59}Co and ^{197}Au,-[6,7] which is given by the equation below.

$$\log\left[\bar{\sigma}(Cf)/\bar{\sigma}(U)\right]=0.0635E_T-0.272. \quad (2)$$

But almost all the data points for the other measured values deviate from the line downward.

So, we again obtained the similar plots using evaluated data values[8]. A line indicated by (2) is the best fit line to these data points, which is given by the equation below.

$$\log\left[\bar{\sigma}(Cf)/\bar{\sigma}(U)\right]=0.0392E_T-0.0680. \quad (3)$$

In this case, the data points for the measured values distribute around the line. So that, we used Eq. (3) to obtain $\bar{\sigma}$(Cf) from $\bar{\sigma}$(U).

In Table 1, values of the data used and the calculated $\bar{\sigma}$(U) and $\bar{\sigma}$(Cf) of nuclei with $t \leq 2$ are shown, the calculated $\bar{\sigma}$(Cf) were obtained from the values of $\bar{\sigma}$(U) labeled by symbol "‡" using Eq. (3). The calculated $\bar{\sigma}$(U) of ^{12}C and ^{16}O are in good agreement with their data values by Calamand. Besides, the values of $\bar{\sigma}$(Cf) of ^{19}F and ^{58}Ni, calculated by Eq. (3) using the data value of $\bar{\sigma}$(U) of ^{19}F and also the two calculated values of ^{58}Ni are close to those by Mannhart. So that, the specrum shape assumed for the U-235 is to be appropriate and hence that of the Cf-252 gives larger values than the actual ones at high energy region. So, Eq. (3) should be valid for calculating $\bar{\sigma}$(Cf) from $\bar{\sigma}$(U).

3. Estimations of unkown cross sections

Fig. 2 shows plots of $25\bar{\sigma} A^{-2/3} E_T^{-1/2}$ calculated using the values of $\bar{\sigma}$(U) labeled by symbol "#" in Table I against E_T values. Values of α and β of the best fit lines to the data points for t=0 and 1 were obtained. Similarly, values of α and β of the best fit line to the data points plotted similarly in Fig. 2 using the values of $\bar{\sigma}$(Cf) in Table I were obtained.

The cross section values estimated by Eq. (1) using the values of α and β are tabulated in Table II, along with confidence intervals estimated under confidence level of 90%. The intervals for t=0 were omitted, because of the small number of the data used. The data points for t=2 are scattered within the narrow interval of E_T value, as seen in Fig. 2, so, these were discarded.

References

1) O. Horibe, Ann. nucl. Energy, 10, pp. 359-373 (1983).
2) Q. J. Hughes, Pile Neutron Research. Addison-Wesley, Massachusetts (1953).
3) A. Calamand, Handbook on Nuclear Activation Cross--sections, pp.299-300. IAEA, Vienna. (1974).
4) W. Mannhart, Proc. 5th ASTM-Euratom Symp. on Reactor Dosimetry Vol. 2, p.801. D. Reidel Publ. Co. (1985).
5) M. Bormann, H. Neuert and W. Scobel, Handbook on Nuclear Activation Cross-sections, pp.213-228. IAEA, Viena. (1974).
6) K. Kobayashi and I. Kimura, INEANDC(J)-67, pp.42-43 (1980).
7) W. L. Zijp, ECN-70 (1979).
8) IRDF-82. IAEA-NDS-41/R (Rev. 0) 1982.

Table I. Basic data and calculated values

Target	E_T (MeV)	U-235 data: Calamand (μb)	U-235 data: Calcul. (μb)	CF-252 data: Mannhart (μb)	CF-252 data: Calcul. (μb)
^{12}C	20.28	$(4.2+1.4)e^{-4}$#	$4.574e^{-4}$		$2.241e^{-3}$#
^{14}N	11.31		1.123#		2.666#
^{16}O	16.65	$(5.3+2.4)e^{-3}$#	$5.444e^{-3}$		$2.037e^{-2}$#
^{9}Be	1.85	$(144+6)e^{3}$#			$144.5e^{3}$#
^{19}F	10.98	7.3+0.7#		16.16(3.4%)#	16.82
^{23}Na	12.96	2.2+0.2	$9.402e^{-1}$#		2.590#
^{39}K	13.42		$5.342e^{-1}$#		$1.534e^{-1}$#
^{46}Ti	13.48	7.8+0.9	4.320#		12.47#
^{50}Cr	12.27	6+1	1.967#		5.538#
^{54}Fe	13.63	5+2.5	1.538#		4.502#
^{58}Ni	12.41	4.9+1.4#	3.966 3.457	8.961(3.59%)#	1.040 9.027

#, these data used as basis of the predictions.
$e^{-4}=10^{-4}$, for example.

Table II. Numerical values of $\bar{\sigma}$ estimated for the (n,2n) cross sections of target nuclei with t=0 and 1.

Samples: Z	Samples: Element	E_T(MeV)	U-235: Experiment (mb)	U-235: Estimated $\bar{\sigma}$ (mb)	U-235: Estimated $\pm\Delta\bar{\sigma}/\bar{\sigma}$ (%)*	Cf-252: Experiment (mb)	Cf-252: Estimated $\bar{\sigma}$ (mb)	Cf-252: Estimated $\pm\Delta\bar{\sigma}/\bar{\sigma}$ (%)*
3	^{6}Li	6.41		3.37e-2			4.60e-2	
5	^{10}Be	9.28		4.15e-3			7.65e-3	
6	^{12}C	20.28	(4.2+1.4)e-7	3.04e-7		(2.241e-6)‡	1.17e-6	
7	^{14}N	11.31	(1.123e-3)‡	9.01e-4		(2.666e-3)‡	2.05e-3	
8	^{16}O	16.65	(5.3+2.4)e-6	9.14e-6		(2.037e-5)‡	3.64e-5	
10	^{20}Ne	17.71		4.16e-6			1.85e-5	
12	^{24}Mg	17.22		7.24e-6			3.06e-5	
14	^{28}Si	17.97		4.14e-6			2.18e-5	
16	^{32}S	15.56		3.79e-5			1.35e-4	
18	^{36}A	15.68		3.69e-5			1.33e-4	
20	^{40}Ca	16.02		2.94e-5			1.09e-4	
3	^{7}Li	8.29		9.07e-2	(+83, -45)		1.62e-1	(+84, -46)
4	^{9}Be	1.85	144+6	1.45e+2	(+112, -53)	(144.5)‡	1.45e+2	(+113, -53)
5	^{11}B	12.5		8.27e-4	(+85. -46)		2.16e-3	(+87, -46)
6	^{13}C	5.33		4.26	(+92, -48)		5.82	(+93, -48)
7	^{15}N	11.56		3.13e-3	(+83, -45)		7.05e-3	(+84, -46)
8	^{17}O	4.39		1.48e+1	(+96, -49)		1.86e+1	(+93, -49)
9	^{19}F	10.98	(7.3+0.7)e-3	7.30e-3	(+83, -45)	(1.613)e-2[m]	1.66e-2	(+84, -46)
10	^{21}Ne	7.08		7.78e-1	(+86, -46)		1.24	(+87, -46)
11	^{23}Na	12.96	(2.2+0.2)e-3	7.80e-4	(+87, -46)	(2.590e-3)‡	2.12e-3	(+88, -47)
12	^{25}Mg	7.63		4.59e-1	(+84, -46)		7.73e-1	(+85, -46)
13	^{27}Al	13.54		4.33e-4	(+89, -47)		1.24e-3	(+90, 47)
14	^{29}Si	8.77		1.33e-1	(+82, -45)		2.48e-1	(+83, -46)
15	^{31}P	12.70		1.30e-3	(+86, -56)		3.45e-3	(+87, -47)
16	^{33}S	8.91		1.23e-1	(+82, -45)		2.32e-1	(+97, -49)
17	^{35}Cl	13.01		9.72e-4	(+87, -47)		2.66e-3	(+88, -47)
19	^{39}K	13.42	(5.342e-4)‡	6.39e-4	(+88, -47)	(1.534e-3)‡	1.81e-3	(+89, -47)

*, confidence interval estimated under 90% confidence level.

‡, our estimated values given in Table I.

m, evaluated value by Hannhart.

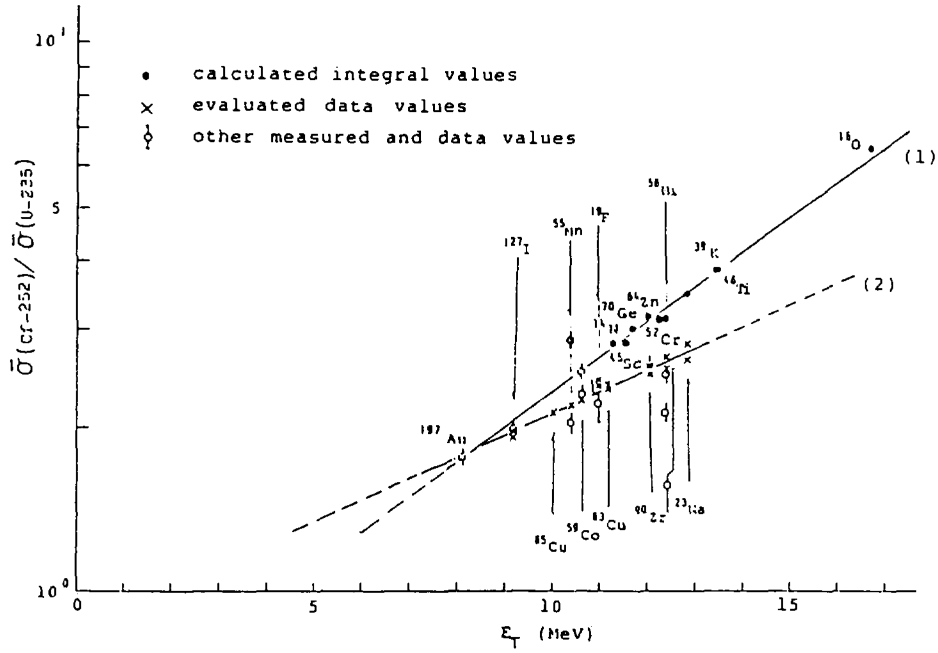

Fig. 1. Plots of log[$\bar{\sigma}$(Cf)/$\bar{\sigma}$(U)] as a function of E_T. A line (1) best fitted to the data points for the calculated $\bar{\sigma}$(Cf) and $\bar{\sigma}$(U) and also measured values on ^{197}Au and ^{59}Co (upper). A line (2), for the spectra averaged cross sections evaluated by NBS for the Cf-252 and U-235 fission spectra and for ENDF/B-V data for the U-235 fission one. Among data points for measured values, those for ^{19}F and ^{58}Ni (lowest) were obtained from the data values by Mannhart and Calamand.

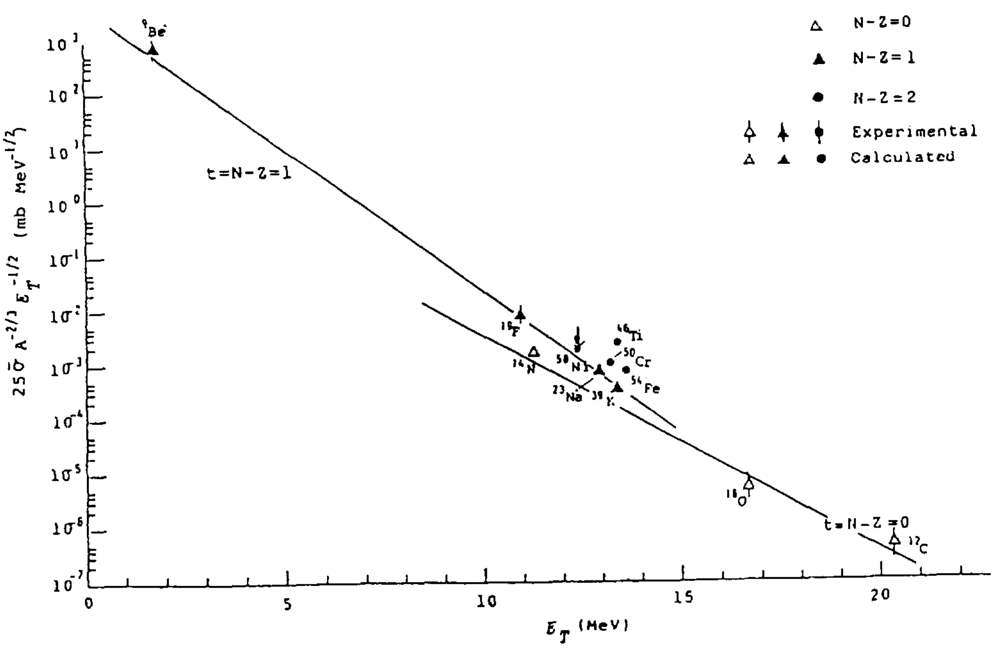

Fig. 2. Plots of log(25 $\bar{\sigma}$ $A^{-2/3}E_T^{-1/2}$) as a function of E_T for the U-235 $\bar{\sigma}$. For the numerical values of $\bar{\sigma}$, see Table I.

IV. Kyushu University

Department of Nuclear Engineering

Faculty of Engineering

IV-1

Shell and Odd-even Effects on Alpha-particle Energy Spectra from (p,α) Reaction on Nuclei around Neutron Number 50

I. Kumabe, Y. Mito, M. Hyakutake, N. Koori

H. Sakai and Y. Watanabe

A paper on this subject was published in Physical Review C 35 (1987) 467-478 with the following abstract :

The energy spectra of α particles emitted from (p,α) reactions on ^{90}Zr, ^{92,94,96,98,100}Mo, ^{93}Nb, ^{106}Pd, and Ag with 18 MeV protons and on some of them with 15 MeV protons have been measured in order to clarify the shell and odd-even effects in the preequilibrium processes of (p,α) and (n,α) reactions. From the experimental results, it was found that there exists no appreciable odd-even effect on the target nuclei in energy spectra for the preequilibrium (p,α) reaction except for the spectra corresponding to the low lying states of the residual nuclei. Considerable change in the energy spectra in the energy region higher than 16 MeV has been observed for target nuclei around the magic number N=50. We have calculated the energy spectra, by using

the knockout model introducing effective Q values, the pairing correlation and a modified uniform spacing model in which the uniform spacing levels have a wide spacing at the magic number. The shell effect of the gross structure of the energy spectra for the nuclei near the magic nuclei can be explained very well in terms of the present knockout model, although the fine structures of the spectra above 16 MeV which correspond to the low lying states or groups of the states of the residual nuclei cannot be explained so well.

IV-2 (p,np) and (p,2p) Reactions Emitting Sub-Coulomb-Barrier Protons

N. Oda, I. Kumabe, M. Hyakutake, N. Koori,

Y. Watanabe, K. Akagi, A. Iida and J. Yano

Grimes et al.[1] have observed large sub-Coulomb-barrier peaks in the energy spectra of protons emitted from 14 MeV (n,xp) reactions on ^{27}Al and others, when for these target nuclei the proton binding energy is less than the neutron binding energy and (n,2n) reaction is energetically inhibited. Since in these cases only available decay channels are sub-Coulomb-barrier proton emission and γ decay, the γ-decay widths can be obtained.

In general, accurate experimental data are available for the reaction induced by charged particles than those for neutron induced reactions because of better counting statistics for reactions related to the charged particles. Moreover the energy of incident charged particles can easily be varied.

In the present experiment we have measured systematically and accurately the double differential cross sections of the (p,p'), (p,np) and (p,2p) reactions which are analogous to the (n,n'), (n,np) and (n,2p) reactions in order to obtain the γ-decay widths from the comparison between the measured and calculated cross sections of sub-Coulomb barrier peaks.

Proton beams from the tandem Van de Graaff accelerator at Kyushu University were analyzed by a beam analyzing magnet and brought into a scattering chamber. A proton detecting system was mounted on a turntable inside the scattering chamber. The detecting system consisted of a ΔE-E counter telescope of three silicon surface barrier detectors. Emitted protons were identified and separated from other reaction products by means of a particle identifier. Incident proton energies were chosen in which large sub-Coulomb-barrier peaks were observed. The proton spectra were measured at the angles ranging from 30° to 165° in steps of 15° .

The experimental and calculated angle-integrated energy spectra for ^{90}Zr, ^{92}Mo, ^{94}Mo, ^{54}Fe and ^{60}Ni are shown in Fig.1. The histograms show the experimental energy spectra and the dotted curves show the calculated energy spectra for the sub-Coulomb-barrier protons. From the present analysis γ-decay widths for ^{90}Nb, ^{92}Mo, ^{92}Tc, ^{94}Tc, ^{54}Fe and ^{60}Cu in the excitation energy corresponding to the neutron binding energy were obtained to be 0.28, 0.36, 0.31, 0.55, 15.0 and 15.5 eV, respectively.

The authors would like to thank the staff of Tandem Accelerator Laboratory for their help in operation of the machine.

References

[1] S.M. Grimes, R.C. Haight and J.D. Anderson, Nucl. Sci. and Eng. 62 (1977) 187, Phys. Rev. C17 (1978) 508; S.M. Grimes, R.C. Haight, K.R. Alvar, H.H. Barshall and R.R. Borchers, Phys. Rev. C19 (1979) 2127.

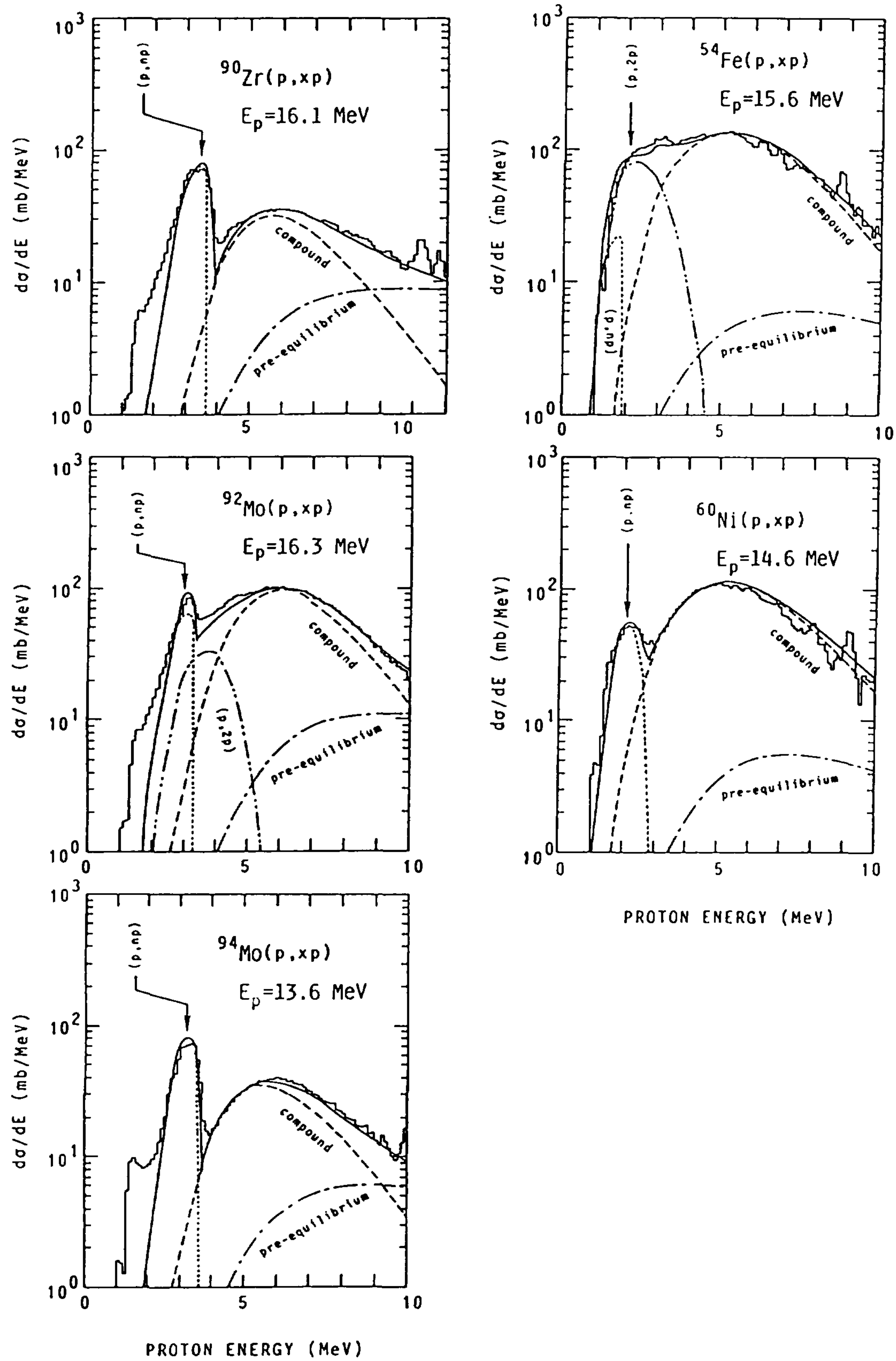

Fig.1 The experimental and calculated angle-integrated energy spectra of protons

IV-3

MEASUREMENTS OF ^{7}Li(p,p'), (p,d) AND (p,t) REACTIONS INDUCED BY POLARIZED PROTONS OF 12, 14 AND 16 MEV

N. Koori, I. Kumabe, M. Hyakutake**, K. Orito+, K. Akagi+,
Y. Watanabe, K. Ogawa+, N. Oda++, J. Yano, A. Iida,
K. Sagara*, H. Nakamura*, K. Maeda*,
T. Nakashima* and M. Kamimura*

Nuclear data for ^{6,7}Li isotopes are important for the fusion reactor development. Especially, tritium production cross sections and double differential cross sections (DDX) for inelastic scatterings are related to the tritium breeding ratio in the reactor and neutron transport in the reactor blanket. It is highly necessary to establish nuclear theories of reactions involving lithium isotopes for the nuclear data evaluation. In order to study adoptability of theories, such as the coupled discretized-continuum channel (CDCC) calculation[1], the Faddeev approach, etc., for the reactions, precise double differential cross sections and analyzing powers were measured for proton induced reactions on ^{7}Li, which have advantages in precision against neutron induced reactions.

Polarized and unpolarized proton beams from the tandem accelerator at Kyushu University were used for measurements of

* Department of Physics, Faculty of Science, Kyushu University.
** Present address: Sasebo Technical College.
+ Present address: Mitsubishi Electric Co.
++ Present address: Toshiba Co.

^{7}Li(p,p'), (p,d) and (p,t) reactions at incident energies of 12.0, 14.0 and 16.0 MeV. Emitted particles were detected with a counter telescope, which consisted of 15.5μm and 75μm thick transmission-type Si detectors and a 2000μm thick Si detector. The lowest energy for the measurement was established to be 1.0 MeV for protons, 1.3 MeV for deuterons and 1.5 MeV for tritons. Protons, deuterons and tritons were separated with a particle identifier. The total energy signals from the identifier were analyzed with a pulse height analyzer (PHA), which had a rooter unit and accumulated simultaneously p, d and t events in separate memory areas. The beam polarization was monitored at the down stream of the scattering chamber with a polarimeter developed by Sagara et al.[2]

The differential cross sections and analyzing powers of ^{7}Li+p scatterings for 12, 14 and 16 MeV were measured for the ground(3/2-), 1st excited (0.478MeV, 1/2-), and 2nd excited (4.63MeV, 7/2-) states. The experimental data of the elastic scattering are excellently reproduced by calculations based on the spherical optical model and the coupled channel (CC) method. The DWBA and CC calculations do not predict correctly the analyzing powers in the inelastic channels leading to the 1st and 2nd excited states of ^{7}Li.

The proton continuum spectrum is mainly due to the ^{7}Li(p,p')tα three-body breakup reaction. Instead of complete CDCC calculations, we tried to calculate the spectrum in the framework of the DWBA by use of the ^{7}Li form factors extended to resonant and non-resonant continuum states. The form factors were obtained on the basis of a microscopic t-α cluster model by Sakuragi et al.[3] The resonant components of the 2nd and 3rd excited states were spread with widths of 0.1 MeV and 1.0 MeV, respectively. The calculated spectra were fitted with optimized normalization factors. The results are compared with the measured one for 14 MeV in Fig. 1. The non-resonant breakups are presented by a dashed line and the total breakups including resonant ones through the $7/2^-$ and $5/2^-$ excited states by a solid line in the figure. Good agreements are indicated in rather wide region except the low energy region. The DWBA calculation with the form factors for discretized-continuum states explains qualitatively the measured continuum spectra.

Triton spectra were calculated by means of the final

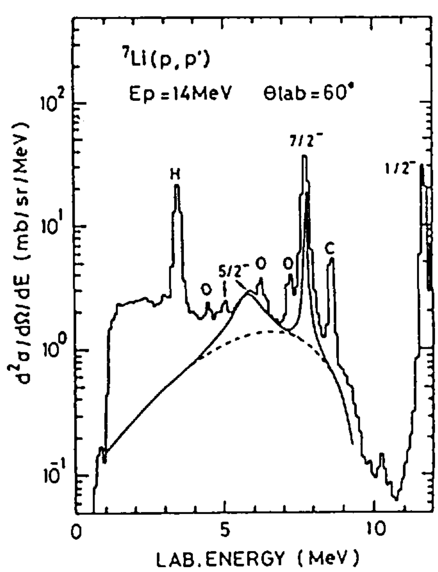

Fig. 1.
Comparison of theoretical calculations by DWBA with a measured proton continuum spectrum for 14 MeV.

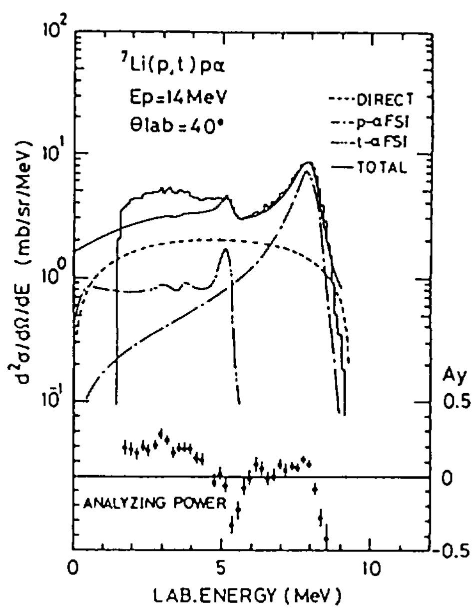

Fig. 2.
Comparison of theoretical calculations by FSI theory with a measured triton spectrum for 14 MeV.

state interaction (FSI) theory, which included only the p-α and t-α FSI and direct-breakup processes as main contributions. The p-wave (3/2) phase shift for p-α scattering and the f-wave (7/2) phase shift for t-α scattering were taken into account in the calculation. The contribution from direct three-body breakup was assumed to be proportional to the phase space factor. These three contributions were added incoherently so as to give good fits with the measured spectra. Fig. 2 shows an example of comparisons for 14 MeV, and suggests that these typical processes are rather independent in the ^{7}Li(p,t)pα three-body breakup reaction. Analyzing powers of the spectra, as shown in the figure, indicate rather large asymmetries at the FSI regions; they can not be predicted in the framework of FSI theory.

More detailed description is available as an internal report.

References

[1] M. Kamimura, Y. Sakuragi, M. Yahiro and M. Tanifuji, J. Phys. Soc. Jpn. Suppl. 55 (1986) 205.

[2] K. Sagara, K. Maeda, F. Hamasaki, H. Nakamura and T. Nakashima, Tandem Acc. Lab. Report, Kyushu University (1985)

[3] Y. Sakuragi, M. Yahiro and M. Kamimura, Prog. Theor. Phys. 70 (1983) 1047.

IV-4

PREEQUILIBRIUM (n,n') SPECTRA FOR NUCLEI AROUND PROTON NUMBER 50

Y. Watanabe, I. Kumabe, M. Hyakutake, A. Takahashi*,

H. Sugimoto*, E. Ichimura* and Y. Sasaki*

Recently we have measured systematically and accurately double differential cross sections of 18 MeV (p,p') scattering from the nuclei around neutron number 50, in order to investigate the shell and odd-even effects in the preequilibrium process on (p,p') scattering[1]. It was found that there were no appreciable shell and odd-even effects on the preequilibrium proton spectra corresponding to excitations above 4 MeV of the residual nucleus. In the present work, we have undertaken to measure the double differential cross sections of the (n,n') scattering, which is analogous with the (p,p') scattering, in order to compare with the results from 18 MeV (p,p') scattering.

The experiment was performed at an incident neutron energy of 14.1 MeV using an 85° TOF facility at OKTAVIAN. The details of this facility and the experimental procedures are described elsewhere[2]. Measurements were carried out for Ag, Cd, In, Sn, Sb, and Te, which are natural elements around proton number 50. Each scatterer was a cylindrical sample of about 3 cm in diameter and about 5 cm long. DDX data for In were taken at 9 angle points between 20° and 160°. However the energy spectra for the remaining samples were measured only at 70° with a longer data accumulation time than that for In. The effects of finite sample size were corrected using multiple scattering correction code MUSCC3[3] in data processing.

Double differetial neutron emission cross sections measured at 70° are shown for Ag, Cd, In, Sn, Sb and Te in Fig.1. In the energy region of 5-10 MeV of interest, where the preequilibrium emission is dominant, the shape

* Department of Nuclear Engineering, Osaka University.

of spectra is identical within errors for all the spectra except for Te. The measured spectrum for Te has such structure that some small peaks overlap, and the magnitude is somewhat larger than those for the other spectra.

In Fig.1, the experimental spectra are compared with $1/4\pi$ of the angle-integrated spectra obtained on the basis of the evaporation and the exciton models, because it was confirmed that the experimental angle-integrated spectrum for In was identical to 4π times the measured spectrum at 70°. In the calculations, the isotope with the mass number almost equal to the atomic weight was assumed as the target nucleus (i.e. ^{107}Ag, ^{112}Cd, ^{115}In, ^{118}Sn, ^{121}Sb and ^{128}Te). The parameter K-value in the exciton model calculation was chosen to be 550 MeV^3. The other parameters are the same as those in the previous (p,p') calculation[1]. As shown in Fig.1, the calculated spectra reproduce the experimental ones well in the outgoing energy region of 1-10 MeV, although an underestimation is seen in 7 to 10 MeV for Te.

Next, to compare the preequilibrium component, the cross sections integrated over 7 to 10 MeV were plotted with respect to the mass number of target nuclei as shown in Fig.2. The cross sections increase monotonically with increasing mass number from Ag to Sb. However the cross section for Te increases discontinuously. As an interpretation on this experimental results, we can suggest the possibility of the excitation of low energy octupole resonance(LEOR) by direct reaction process.

In a systematic investigation on LEOR[4], it has been shown that excitations of LEOR are not appreciably observed if the strong transition to the first 3^- state occured. From comparisons of the deformation parameter β_3 for the first 3^- deduced from (n,n'),(p,p') and (α,α') scatterings, it was found that β_3 values for ^{128,130}Te are smaller than those for the others.[5] We estimated the deformation parameter β_{LEOR} for

LEOR under the assumption that the EWSR fraction for LEOR plus the first 3^- state is 30 % and the excitation energy of LEOR is $31A^{-1/3}$, where A is the mass number. Following the direct reaction theory, the cross section for excitations of LEOR was predicted from the expression $\beta_{LEOR}{}^2 \cdot \sigma_{DW}$, where σ_{DW} is the DWBA cross section. The predicted LEOR cross section for Te was 20-45% larger than those for the other nuclei. The cross sections after subtraction of the LEOR cross section from the experimental ones are shown by open circles in Fig.2. Compared with the experimental cross sections(solid circles), these cross sections increase monotonously within errors with an increase in the mass number. This component would be considered to be the preequilibrium component, because excitations of the coherent motion such as LEOR can not be well explained in the framework of the preequilibrium model such as the exciton model.

Therefore, it was confirmed that the shell and odd-even effects were not appreciably observed in the preequilibrium process on the (n,n') scattering as well as the (p,p') scattering.

References

[1] Y. Watanabe et al., to be submitted to Phys. Rev. C.

[2] A. Takahashi et al., Proc. Int. Conf. Fast Neutron Physics, Dubrovnik, May 26-31, 1986 (Ruder Boskovic Institute Pub. 1986).

[3] E. Ichimura et al., OKTAVIAN Report A-87-02.

[4] J.M. Moss et al., Phys. Rev. C 18, 741 (1978).

[5] W. Makofske et al., Phys. Rev. 174, 1429 (1968).

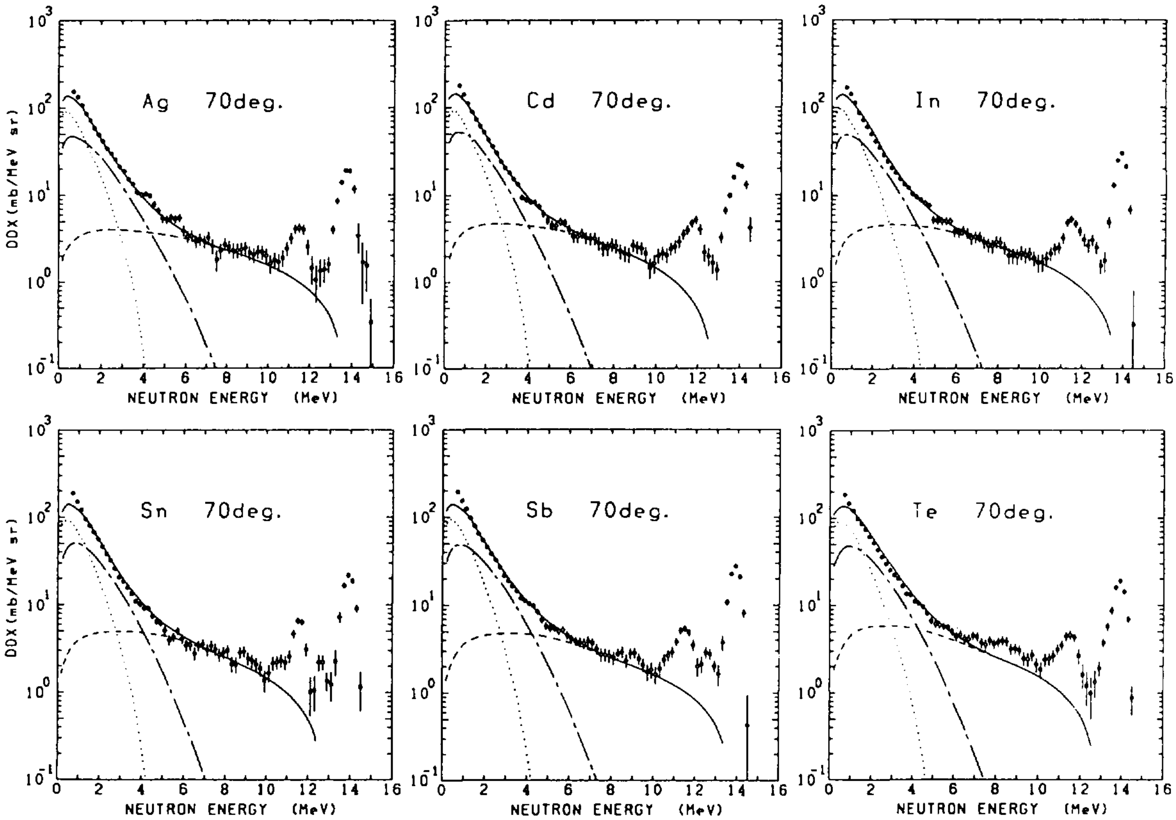

Fig. 1. Comparisons of the experimental and calculated double differential neutron emission cross sections for Ag, Cd, In, Sn, Sb, and Te. Dashed curves are the calculated preequilibrium spectra using the exciton model. Dotted-dashed curves and dotted curves show the calculated evaporation spectra for the emission of one neutron and two neutrons, respectively. Solid curves are the sum of them.

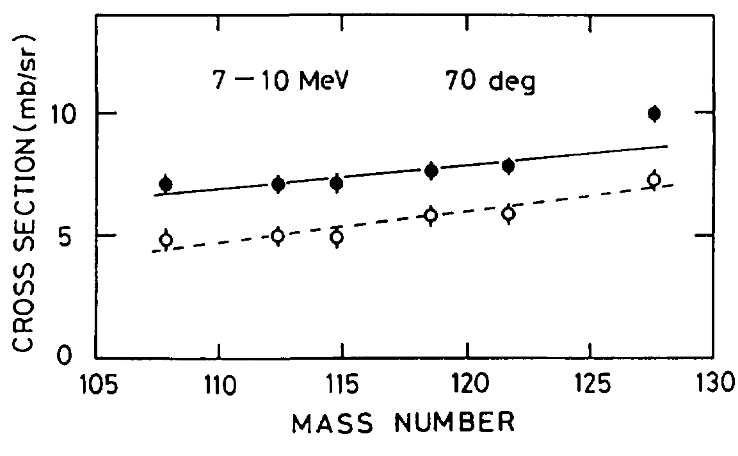

Fig. 2. Dependence of integrated cross sections over 7 to 10 MeV on the mass number of target nuclei. Solid circles represent the measured cross sections at 70°. Open circles are the results after subtraction of the predicted LEOR component.

V. NAGOYA UNIVERSITY

Department of Nuclear Engineering

Faculty of Engineering

V-1 Decay of ^{143}La and ^{145}Ce

H. Ukon, M. Shibata, K. Kawade, H. Yamamoto,

T. Katoh, Y. Kawase*, K. Okano*, J-Z. Ruan**

Decay studies of ^{143}La and ^{145}Ce were made at the On-line Isotope Separator Facility (KUR-ISOL) of Kyoto University. The sources of ^{143}La and ^{145}Ce were separated from fission products of ^{235}U irradiated at the Kyoto University Reactor. The gamma-ray singles, gamma-gamma cioncidence, and beta singles measurements were performed by using two Ge detectors and a LEPS.

1. Emission rate of the 620 keV gamma-ray in the decay of ^{143}La

The emission rate of the 620 keV gamma-ray was determined. The gamma-ray intensity was compared with the intensity of the 293 keV gamma-ray in the decay of ^{143}Ce, which was 42.8±0.4 percent. The present result of the emission rate of the 620 keV gamma-ray is 4.41±0.33 percent and is larger than that of Blachot et al.

---

* Research Reactor Institute, Kyoto University

** Rikkyo University

2. Decay energy of ^{143}La and ^{145}Ce.

The beta end point measurements of ^{143}La and ^{145}Ce were made by using a LEPS. The end points were determined from the Fermi-Kurie analyses of beta spectra. Preliminary results of the end point energies of ^{143}La and ^{145}Ce are 3361 and 1736 keV, respectively.

3. Decay scheme of ^{143}La and ^{145}Ce

Decay schemes of ^{143}La and ^{145}Ce were constructed from the present experiments. For decay of ^{143}La, thirty-six levels (new levels at 808.8, 1880.2, 2815.7, 2848.1, 2867.2, 2896.9, 2988.3 and 3056.1 KeV) of ^{143}Ce are proposed and eighty-six gamma-rays are incorporated in this decay scheme. For decay of ^{145}Ce, thirty-six gamma-rays (seven new gamma) are incorporated in the decay scheme as shown in Fig. 1.

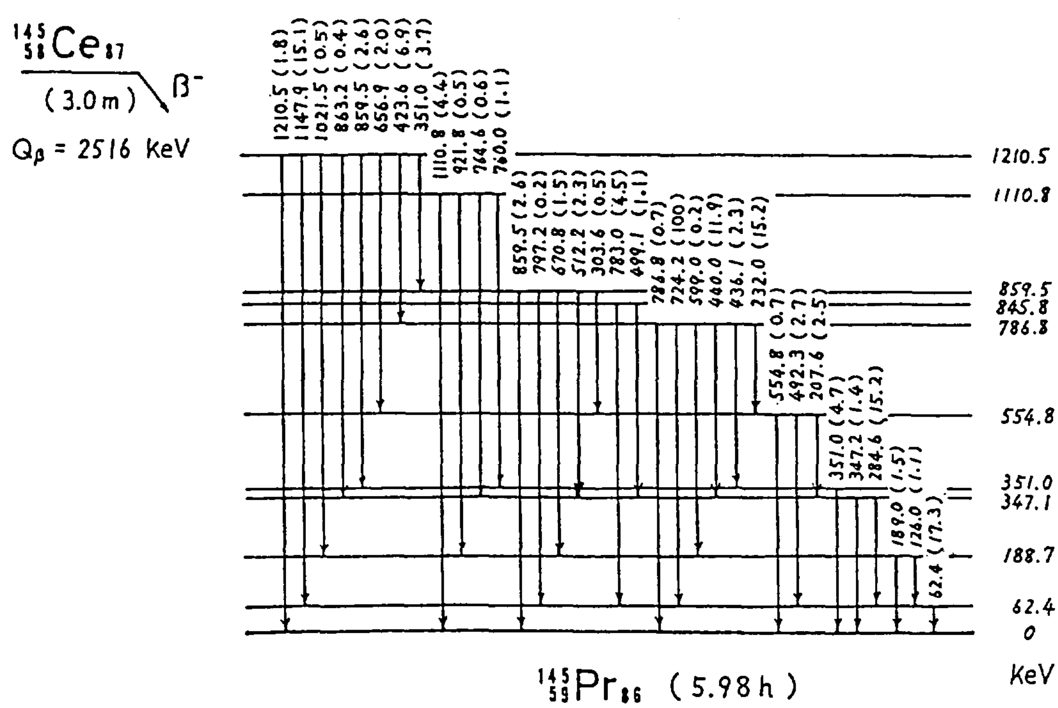

Fig.1 A decay scheme of ^{145}Ce

V-2 Measurement of 14 MeV Neutron Activation Cross-sections of Fusion Reactor Materials

T. Katoh, K. Kawade, H. Yamamoto, M. Shibata,
H. Ukon, M. Miyachi, A. Takahashi* and T. Iida*

Measurement of 14 MeV neutron activation cross-sections of fusion reactor materials have been done to provide the basic data for the assessment of damage and activation of materials due to the high flux fast neutron.

1. Cross-sections of $^{27}Al(n,p)^{27}Mg$ and $^{63}Cu(n, 2n)^{62}Cu$ reactions.

The $^{93}Nb(n,2n)^{92m}Nb$ reaction has been used for a monitor reaction of the neutron flux measurement. However, when the product nuclide is a short-lived one (<10 min.) in case of activation cross-section measurement, the $^{93}Nb(n,2n)^{92m}Nb$ reaction is not a good monitor reaction because of the half-life (10.15d) of ^{92m}Nb. Then, the $^{27}Al(n,p)^{27}Mg(T_{1/2}=$ 9.47m) is considered as a substitute for the monitor reaction, and its cross-sections were measured in this series of experiments.

The aluminum samples (99.2 %, 1 cm x 1 cm x 0.2 mm) were irradiated with the fast neutron by using a pneumatic tube irradiation system at the Intense 14 MeV Neutron Source Facility (OKTAVIAN) of Osaka University. The pneumatic tubes were set at five angle directions for the incident deuteron

* Department of Nuclear Engineering, Osaka University

beam direction. The neutron fluxes at the samples were about 1×10^8 n/cm^2 s and monitored for each sample. The monitor reaction was ^{27}Al(n, α)^{24}Na reaction generated in the same sample. The neutron energy was measured by the Zr-Nb method. The irradiation time were 5, 7 and 9 min. Gamma-rays from produced radioactive elements were measured with a Ge(Li) detector to obtain cross-sections.

Results of the present measurement are shown in Fig. 1 together with previous values. The present results support the estimation of JENDL-2.

By using the present results of the ^{27}Al(n,p)^{27}Mg reaction as a monitor, the activation cross-sections of ^{63}Cu(n,2n)^{62}Cu reaction were measured.

The Cu samples (1 cm x 1 cm x 0.1 mm) were irradiated by the fast neutron with Al foils which were used for monitors. The activity of ^{62}Cu ($T_{1/2}$=9.47m) was estimated by measuring the annihilation gamma-rays.

Results are shown in Fig. 2.

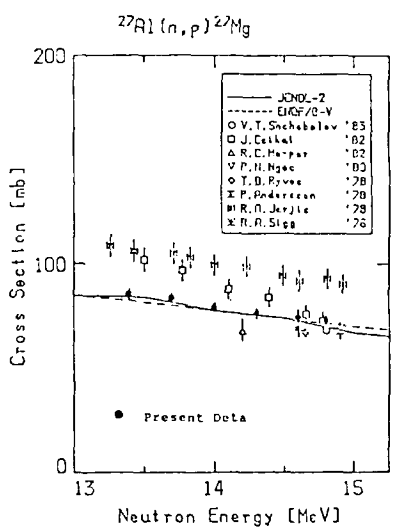

Fig. 1

Cross-sections of ^{27}Al(n.p)^{27}Mg reaction

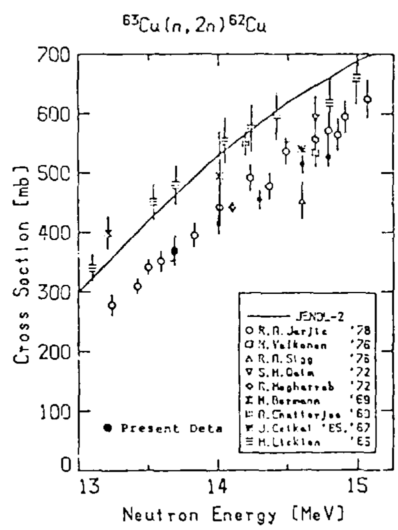

Fig. 2

Cross-sections of ^{63}Cu(n, 2n)^{62}Cu reaction

2. Half-life of ^{24}Na and ^{27}Mg

The method of half-life measurement of short-lived activity was investigated. The application of the pulsar method and the standard source method in case of short-lived activity were studied. The correction method for the pile-up and the dead-time was experimentally established.

By using the results of this study, the half-life of ^{24}Na and ^{27}Mg were obtained as 14.963±0.007h and 9.465±0.015m, respectively.

VI. Tohoku University

Department of Nuclear Engineering

Faculty of Engineering

VI-1

Double-differential Neutron Emission Cross Sections of Ti, Cu, Zr and C for 14.1 MeV Neutrons

M.Baba, T.Kikuchi, M.Ishikawa, H.Wakabayashi and N.Hirakawa

A report on this subject is in press as NETU-49 (Annu.Rep.Fast Neutron Lab., Tohoku Univ.) with the following abstract:

We have measured the energy-angular doubly-differential neutron emission cross sections of titanium, copper, zirconiuum and carbon for 14.1 MeV incident neutrons. The experimental details were reported previously[1,2]. The flight path length was ~4 to 8m, and samples were right cylinders, 4cm long and 2.5cm (Ti, Cu, C) or 3.5cm (Zr) in diameter. In this study, we took account of the backgrounds caused by neutrons scattered around target and collimator. In addition, cares were taken to make a reliable data correction for finite sample size effect.

From the measured data, we derived as well the angle-integrated neutron emission spectra and differential elastic and inelastic scattering cross sections. Typical examples of neutron emission spectra are shown for titanium, copper and zirconiuum in Fig.1, together with the evaluated values. The present data indicate the existence of angle dependent high energy neutrons which were not considered in the evaluation. The angle dependence of these neutrons from zirconiuum was compared with Kalbach-Mann systematics[3] and proved to be followed rather satisfactorily.

The results for carbon were in general agreement with our previous ones[4]. However, these for continuum neutrons resulting from (n,n'3α) reaction are ~30% lower than previous ones and close to the recent values at Osaka university[5] and PTB[6].

References:

1. M.Baba, JAERI-M86-029(1986)pp.119
2. S.Chiba et al., J.Nucl.Sci.Technol., 22 1(1985)
3. C.KalbachandF.M.Mann,Phys.Rev.,C33112(1981)
4. M.Baba et al., Radiation Effects 92-96 223(1986)
5. A.Takahashi, JAERI-M86-080(1986)pp.191
6. B.Antolkovicetal., Proc. Int.Conf., "FastNeutronPhysics"(Dubrovnik,1986)pp.137

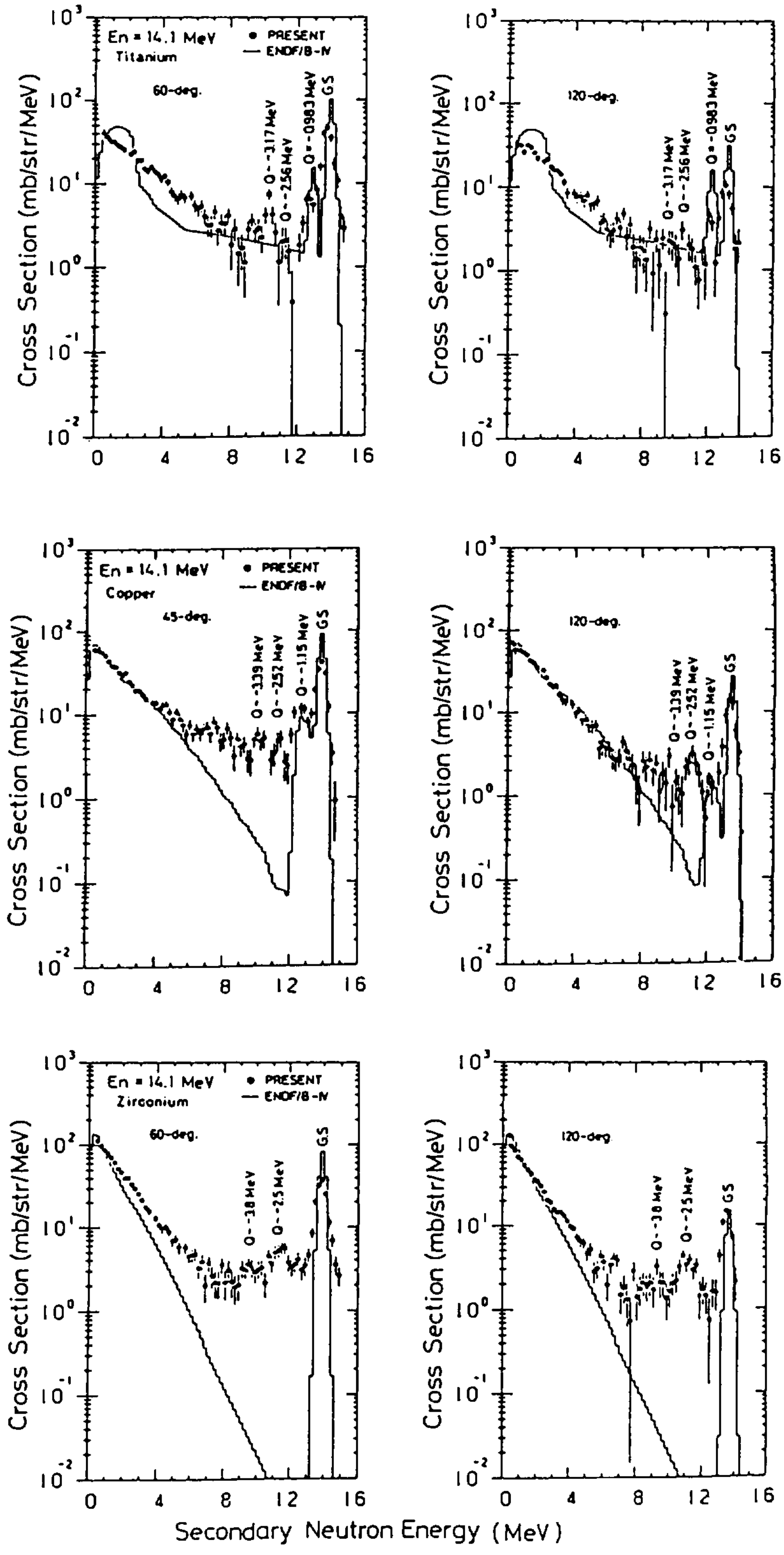

Fig. 1 Double-differential neutron emission cross sections of titanium, copper and zirconiuum.

VI-2 Measurement of Prompt Fission Neutron Spectrum of ^{232}Th

M.Baba, H.Wakabayashi, M.Ishikawa, T.Kikuchi and N.Hirakawa

A report of this subject is in press as NETU-49 (Annu.Rep.Fast Neutron Lab., Tohoku Univ.) with the following abstract:

We have measured the prompt fission neutron spectrum of thorium to reduce the uncertainty in our previous data[1,2] and to extend the energy range of measured spectrum. For the purpose, we adopted an improved experimental apparatus; a larger neutron detector (14cmϕ and 10cm long NE213), longer flight path (3.12m) and better timming resolution for high energy neutrons. The signal to background ratio was much improved as well by raising the detector bias to obtain clear cutoff of γ-rays in a pulse shape discriminator. The detector efficiency and energy scale were calibrated using two independent method. The energy of incident neutrons were 2 MeV with energy spread ~50keV.

The result is shown in Fig.1, compared with the evaluation; these are normalized between 2.2 and 5 MeV. The present result is followed well by the Watt-type spectrum adopted in JENDL-2, but deviates downward from the Maxwellian spectrum in higher energy region. The presently obtained mean energy and Maxwellian temperature of fission neutrons are found to satisfy the relation with ν (number of prompt neutrons per fission) proposed by Howerton and Doyas[3]

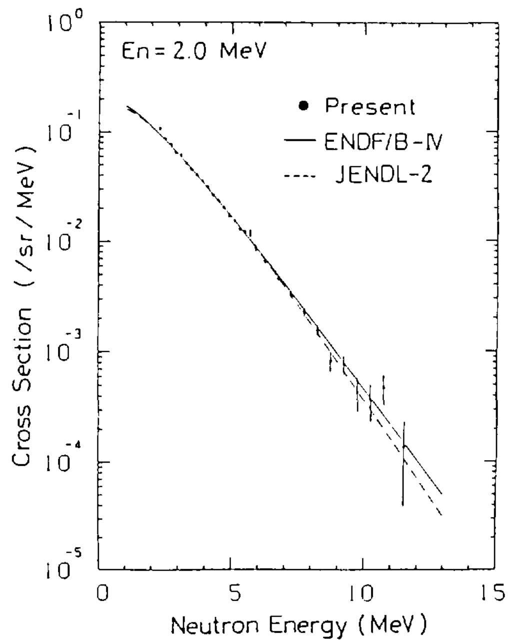

Fig.1 ^{232}Th fission neutron spectrum.

References:

1. H.Nakashima et al., NETU-44 (Dep. Nucl. Eng., Tohoku Univ., 1984) pp.36
2. N.Hirakawa et al., Radiation Effects 92-96 565(1986)
3. R.J.HowertonandR.J.Doyas Nucl.Sci.Eng., 46 414(1971)

VI-3

Measurement of Neutron Induced Fission Cross Sections of ^{233}U relative to ^{235}U from 0.2 to 0.8 MeV

F.Manabe, T.Iwasaki, M.Baba, Y.Karino, S.Matsuyama and N.Hirakawa

A paper on this subject is in press as NETU-49 (Annu.Rep.Fast Neutron Lab., Tohoku Univ.) with the following abstract:

We have measured neutron induced fission cross sections of ^{233}U relative to ^{235}U at the energy range from 0.2 to 0.8 MeV. The method of experiments and data analyses have been described[1,2]. In this study, we newly adopted a time-of-flight technique to reduce the experimental uncertainty due to room-returned neutrons and α-particles background. For the aim, we developed a fast timming fission fragment counting system using an ionization chamber with closely-spaced (~4mm) electrodes and fast timming electronics. The overall timming resolution was ~5 to 8 ns. The source neutrons were produced via the $^{7}Li(p,n)$ reaction with energy spread of ~50keV. The data were analysed considering the correlation between error elements.

The results are shown in Fig.1 together with other experimental and evaluated values. The present data show general agreement with those by Carlson & Behrens, and Meadows, but are consistently higher than the evaluations. Such discrepancies with evaluated data were seen also in higher energy region.[1]

References:

1. K.Kanda et al., Radiation Effect 92-96 569 (1986)
2. K.Kanda et al., J.Nucl.Sci.Technol., 24 423 (1987)

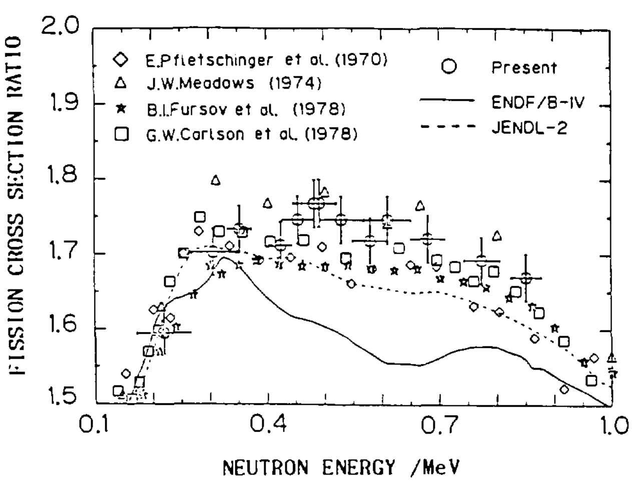

Fig.1 $^{233}U/^{235}U$ fission cross section ratio.

VI-4

Measurement of Neutron Induced Fission Cross Section of ^{235}U around 14 MeV

Y. Karino, T. Iwasaki, F. Manabe, S. Matsuyama, M. Baba, K. Kanda* and N. Hirakawa

A report of this subject is in press as NETU-49 (Annu.Rep.Fast Neutron Lab., Tohoku Univ.) with the following abstract:

The neutron induced fission cross sections of ^{235}U were measured at the incident energy from 13.5 to 14.9 MeV using a low-mass fission chamber coupled with a proton-recoil counter-telescope in back to back form. This cofiguration enables neutron fluence determination with minimal uncertainty. The neutron sensitivity of the recoil proton counter was carefully calibrated using a time-correlated associated-particle (TCAP) method. The experimental result agreed with the calculated one within 1%; this showed the applicability of the counter telescope to high precision neutron fluence determination.

The fission cross section measurements were carried out using the source neutrons produced via the d-T reaction at various emission angle. The fission cross sections were obtained within 2.8 %. The results are shown in Fig. 1. The present results show good agreement with those using TCAP method by Wasson, Cance, Jingwen and Adamov, in magnitude, and with those by Czirr and Kari in energy dependence. This technique will be applied to the measurements in other neutron energies.

---

* Present address: Fujikoshi Co. Ltd., Ishigane, Toyama-shi 930

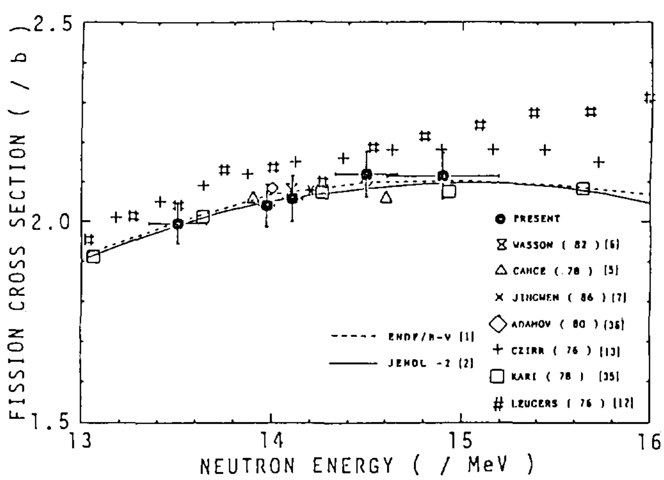

Fig. 1 ^{235}U neutron induced fission cross section.

VI-5

Measurement of Fast Neutron Induced Fission Cross Sections of ^{243}Am relative to ^{235}U

K.Kanda*, H.Imaruoka**, H.Terayama, Y.Karino and N.Hirakawa

A paper on this subject was published in Jour.Nucl.Sci.Technol., 24 423(1987) with the following abstract;

The fission cross section ratio of ^{243}Am to ^{235}U has been measured in the energy range of 1.1 ~ 6.8 MeV with monoenergetic neutrons. An ionization fission chamber was used to detect fission events. The quantitative analyses of the fission samples were made with a low geometry counter and a 2π counter. Uncertainties of the measured data were analyzed considering correlations between error elements. The present result is very close to that of Fursov et al. and lower by about 20% than the values reported by Behrens & Browne.

---

* Present address; Fujikoshi Co. Ltd., Ishigane, Toyama-shi 930.

** Present address; Toshiba Corp., Shinsugita-cho, Isogo-ku, Yokohama 235.

VII. Tokyo Institute of Technology

Research Laboratory for Nuclear Reactors

VII-1 Particle-Vibrator Coupling Model Calculation of Partial Radiative Widths for $p_{3/2}$ Wave Neutron Resonance on ^{28}Si

H. Kitazawa, M. Ohgo, T. Uchiyama, and M. Igashira

A particle-vibrator coupling model was applied to the calculation of partial radiative widths for the ^{28}Si $p_{3/2}$ wave neutron resonance with large reduced neutron width. The calculation assumed a neutron excitation coupled to one-phonon vibrational states of the ^{28}Si nucleus and neglected the continuum nature of the resonance state wave function in the nuclear external region. The model wave functions were generated from a coupled-channel Schrödinger equation so as to reproduce the observed neutron escape width, neutron binding energies, and spectroscopic factors. Excellent agreement was achieved between the observed and calculated partial radiative widths for the transitions from the 565 keV resonance to the low-lying states of ^{29}Si. As a result, it was confirmed that the core excitation is quite essential to explain the observed partial radiative widths. We emphasize that this resonance can be interpreted as a particle-vibrator doorway state common to the neutron and gamma-ray emission channels, and that a dominant component of the doorway-state wave function belongs to the configuration in which a single quasibound $1d_{3/2}$ neutron is coupled to the 3^- vibrational state of the ^{28}Si nucleus.

Published in Nucl. Phys. A464 (1987) 61-74.

VII-2 Systematics and Mechanism of Pygmy E1 Resonance

M. Igashira, H. Kitazawa, and T. Uchiyama

To investigate the pygmy E1 resonance for nuclei with $N \simeq 50 \sim 126$, neutron capture gamma-ray spectra of Nb, Mo, Ag, In, Sn, Sb, I, Cs, Pr, Tb, Ho, Lu, Ta, and Au have been measured with an anti-Compton NaI(Tl) detector in keV-neutron energy region, using a time-of-flight technique. All observed spectra except for Nb and Mo show the anomalous bump, so-called the pygmy resonance. The observed spectra were compared with the statistical model calculations which used the Brink-Axel E1 gamma-ray strength function with a pygmy E1 resonance. The pygmy resonance parameters were extracted from these spectra by a spectrum fitting method, and the systematics of the resonance energy and the E1 strength exhausted in the resonance were obtained as the functions of neutron number. Both the systematics show distinct shell effects at the neutron magic number of N=82 and at the proton magic number of Z=50. Comparison with both shell model and hydrodynamical model predictions for the pygmy E1 resonance indicates that the observed pygmy E1 Resonances, at least in the mass region of $Z= 50 \sim N=126$, have a common physical origin, and that neutron particle-hole states decoupled from the giant E1 resonance would be responsible for these resonances.

Contributed to the 6th International Symposium on Capture Gamma-Ray Spectroscopy, Leuven (1987).

VII-3 Mechanism of s-Wave and p-Wave Neutron Resonance Capture in Light and Medium-Weight Nuclei

H. Kitazawa, and M. Igashira

Capture gamma-ray spectra of light and medium-weight nuclei have been measured to investigate the mechanism of neutron capture on s-wave and p-wave resonances with large reduced neutron width.

Capture gamma-ray spectra of ^{16}O have been observed in our expectation that the high single-particle nature of the ground state ($5/2^+$; 0.0 MeV) and the first excited state ($1/2^+$; 0.87 MeV) of ^{17}O would facilitate the E1 valence transitions from the 434-keV $p_{3/2}$-wave resonance (Γ=45 keV). The results demonstrate that the Lane-Mughabghab valence capture model reproduces successfully the observed partial radiative widths for these transitions.

Observations were also made for gamma-rays from neutron capture on the 565-keV (Γ=12 keV) and 806-keV (Γ=27 keV) $p_{3/2}$-wave resonances of ^{28}Si. The p-wave resonance capture is followed by strong gamma-ray transitions to a small number of low-lying states of ^{29}Si. The valence capture model reasonably accounts for the ground state ($1/2^+$; 0.0 MeV) and second excited state ($5/2^+$; 2.03 MeV) transitions from both p-wave resonances, while other transitions cannot be understood by this model.

A particle-vibrator coupling model was applied to the calculation of partial radiative widths for the $p_{3/2}$-wave resonance of ^{28}Si. The calculation assumed a neutron excitation coupled to one-phonon vibrational states of ^{28}Si and neglected the continuum nature of the resonance state wave function in the nuclear external region. As a result, we found that the core excitation is essential to explain the observed gamma-ray transitions from the p-wave resonances of ^{28}Si and that these transitions are almost decoupled from the giant electric dipole resonance.

The effects of the core excitation in the resonance capture in ^{32}S were investigated with measurements of gamma-rays from the 202-keV $p_{1/2}$-wave resonance (Γ=3 keV). There is also some possibility of the core excitation.

Moreover, strong correlations between spectroscopic factors and partial radiative widths have been observed in the gamma-ray transitions from the 188-keV s-wave resonance (Γ=60 keV) of ^{28}Si and the 103-keV s-wave resonance (Γ=15 keV) of ^{32}S. These correlations are understood in the framework of the extended valence capture model which includes the M1 transition described by the renormalized M1 operator.

Our results will supply a clue for elucidating the physical nature of the particle-core coupling scheme in neutron resonance capture processes.

Contributed to the 6th International Symposium on Capture Gamma-Ray Spectroscopy, Leuven (1987).